

**II Russian-Chinese International School
"Superconducting functional materials for
advanced quantum technologies'24"**

Monday, 23 September -- Friday, 27 September 2024

**BOOK OF
ABSTRACTS**

MIPT

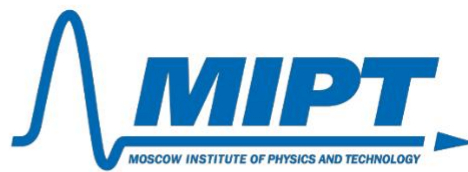
Organizing Committee

Prof. Vasily S. Stolyarov (*Moscow Institute of Physics and Technology*)

Prof. Aleksandr V. Andriyash (*Dukhov Research Institute of Automatics (VNIIA)*)

Prof. Irina V. Bobkova (*Moscow Institute of Physics and Technology*)

Prof. Alexander A. Golubov (*Moscow Institute of Physics and Technology*)



The school was supported by the project “Superconducting functional materials for advanced quantum technologies” (No.23-72-30004) - Grant from the Russian Science Foundation

Monday, September 23, 2024	
Location: Room 119, Main Building, MIPT	
Session Chair: Prof. Irina BOBKOVA	
09:00-09:15	<i>Welcome remarks</i> Prof. Vasily STOLYAROV (MIPT) Andrei BLINOV (Russian Science Foundation' Vice Deputy General) Prof. Alexander GOLUBOV (MIPT)
09:15-10:45	Prof. Anatolie SIDORENKO <i>Brain like artificial neural network based on superconducting elements</i>
10:45-11:00	Coffee Break & Take Photos
11:00-12:30	Prof. Wei JIANG <i>Theoretical study of flat band models and materials</i>
12:30-14:00	Lunch
14:00-15:30	Prof. Alexey ALADYSHKIN <i>Composing of skeletons of 2D images and analysis of SPM data</i>

Tuesday, September 24, 2024	
Location: Room 119, Main Building, MIPT	
Session Chair: Prof. Alexander GOLUBOV	
09:00-10:30	Prof. Yu ZHANG <i>Characterization and Manipulation of Intervalley Scattering in Graphene</i>
10:30-11:00	Coffee Break
11:00-12:30	Prof. Irina BOBKOVA <i>Proximity effect in superconductor/magnet heterostructures</i>
12:30-14:00	Lunch
14:00-15:30	Prof. Yangyang JU <i>Enhanced Study on the Utilization of Trace Gas Sensors for Early Disease Detection</i>

Wednesday, September 25, 2024	
Location: Room 119, Main Building, MIPT	
Session Chair: Prof. Alexey ALADYSHKIN	
09:00-10:30	Prof. Alexander MELNIKOV <i>Superconducting spintronics: interplay between superconductivity and magnetism</i>
10:30-11:00	Coffee Break
11:00-12:30	Prof. Peng LIU <i>Insights into Soft Matter Dynamics and Structure via Three Entropic Effects</i>
12:30-14:00	Lunch
14:00-15:30	Prof. Yangyang JU <i>Enhanced Study on the Utilization of Trace Gas Sensors for Early Disease Detection</i>

Thursday, September 26, 2024	
EXCURSION DAY	

Friday, September 27, 2024	
Location: Room 119, Main Building, MIPT	
Session Chair: Prof. Alexander MELNIKOV	
09:00-10:30	Prof. Quanzhen ZHANG <i>Introduction to advanced science of low dimensional semiconductor materials and nanodevices</i>
10:30-11:00	Coffee Break
11:00-12:30	Prof. Lada YASHINA <i>Characterization of topological insulators and related materials using synchrotron radiation</i>
12:30-14:00	Lunch
14:00-15:30	Prof. Yuhui CHEN <i>Rare Earth-Doped Crystals for Quantum Network Applications</i>
15:30-18:00	Poster Session (UVD, 2nd floor)

Posters

Spin supercurrent in superconductor/ferromagnet van-der-Waals heterostructures	25
Three-Dimensional Multi-Orbital Flat Band Models and Materials	27
Magnetic properties of the $\text{Mn}_{3-x}\text{Ni}_x\text{BO}_5$ Single Crystal	28
Magnon-photon coupling in superconductor/ferromagnet heterostructures.....	29
Magnetic proximity effect in superconductor/ferromagnet van der Waals heterostructures: dependence on the number of superconducting monolayers	30
SnS-Andreev spectroscopy study of superconducting gap structure of $\text{NaFe}_{1-x}\text{Co}_x\text{As}$ compounds.....	31
Mixing entropy engineering	32
Research on Electrochemical Biosensors Based on Topological Materials.....	33
A Universal Strategy for Synthesis of 2D Ternary Transition Metal Phosphorous Chalcogenides.....	34
4 inch Gallium Oxide Field-Effect Transistors Array with High-k Ta_2O_5 as Gate Dielectric by Physical Vapor Deposition.....	35
The local electronic structure of the antiferromagnet CeCo_2P_2 exhibiting the Kondo effect	36
Defect engineering in monolayer transition metal dichalcogenides	38
Surface spin-flop in antiferromagnetic topological insulator $\text{Ge}_{0.4}\text{Mn}_{0.6}\text{Bi}_2\text{Te}_4$	39
Influence of capacitance and thermal fluctuations on the Josephson diode effect in asymmetric higher-harmonic SQUIDs	40
Magnetic properties of the $(\text{Mg}_{1-x}\text{Ni}_x)_3\text{Si}_2\text{O}_5(\text{OH})_4$ $x=2/3$ and 1	41
$0-\pi$ transition in planar Josephson S-N-S junction on a ferromagnetic insulator substrate ...	42
Synthesis and properties of materials based on mixed manganese, indium and bismuth tellurides	43
Two-dimensional Ferrovalley Semi-Half-Metal and Tunable Valley-Unbalanced Quantum Anomalous Hall Effect.....	44
Microwave generator based on the Josephson junction	45
A new Mn-Bi-Te ternary antiferromagnetic topological insulator.....	47
Nanoscale visualization of symmetry-breaking electronic orders and magnetic anisotropy in a kagome magnet YMn_6Sn_6	48
Intertwined quantum confinement effects in charge-density-wave nanostructures	49
Crystal growth of topological insulators with bulk-insulating property.....	50
Vortex glass – vortex liquid phase transition in the iron-based superconductor $\text{PrFeAs}(\text{O},\text{F})$	51

Implementation of a fast qubit reset algorithm on a superconducting transmon	52
Design of a transmon qutrit scheme for quantum magnetometry	54

Contents

Lectures

Composing of skeletons of 2D images and analysis of scanning-probe-microscopy data..... 12

Aladyshkin A.Yu.

Rare Earth-Doped Crystals for Quantum Network Applications 13

Chen Yuhui

Proximity effect in superconductor/magnet heterostructures 14

Bobkova I.V.

Electrodynamic properties of superconductors: fundamentals and experimental approaches
..... 15

Gorshunov B.P.

Theoretical study of flat band models and materials..... 16

Jiang Wei

Enhanced Study on the Utilization of Trace Gas Sensors for Early Disease Detection 17

Ju Yangyang

Insights into Soft Matter Dynamics and Structure via Three Entropic Effects 18

Liu Peng

Superconducting spintronics: interplay between superconductivity and magnetism..... 19

Melnikov A.Yu.

Brain like artificial neural networks based on superconducting elements 20

Sidorenko A.S.

Characterization of topological insulators and related materials using synchrotron radiation
..... 21

Yashina L.V.

Characterization and Manipulation of Intervalley Scattering in Graphene 22

Zhang Yu

Controllable Construction and Electronic Properties Investigation of Low-Dimensional
Materials by SPM 23

Zhang Quanzhen

LECTURES

Composing of skeletons of 2D images and analysis of scanning-probe-microscopy data

Alexey Yu. Aladyshkin^{1-3,*}

¹Institute for Physics of Microstructures RAS, Nizhny Novgorod, Russia

²Center for Advanced Mesoscience and Nanotechnology,

³Lobachevsky State University of Nizhny Novgorod, Nizhny Novgorod, Russia *email: aladyshkin@ipmras.ru

This lecture is devoted to the composing of skeletons of two-dimensional (2D) halftone images for further analysis. The introductory part of the lecture is aiming to meet audience with a powerful technique of skeletonization [1]. The skeleton is a combination of one-pixel-wide lines (continuous or broken) which reproduce topology and peculiar shapes of an original halftone image. In order to plot a skeleton for given image one can use built-in functions (for example, in the programming languages Matlab and Python), or compose independently considering cross-sectional views line-be-line. The latter case is applicable even for noisy images with pronounced gradient of contrast. The skeleton can be used for automatic determination of peculiar points like branching and end points (see Fig. 1). To illustrate capability of this approach we consider problems of determination of edges of atomically-flat terraces, screw dislocations, fingerprint identification etc. The original part of the lecture is devoted to numerical analysis of motion of topological defects for a series of noisy images acquired by magnetic-force microscopy for $\text{EuFe}_2(\text{As}_{1-x}\text{P}_x)_2$ single crystals [2].

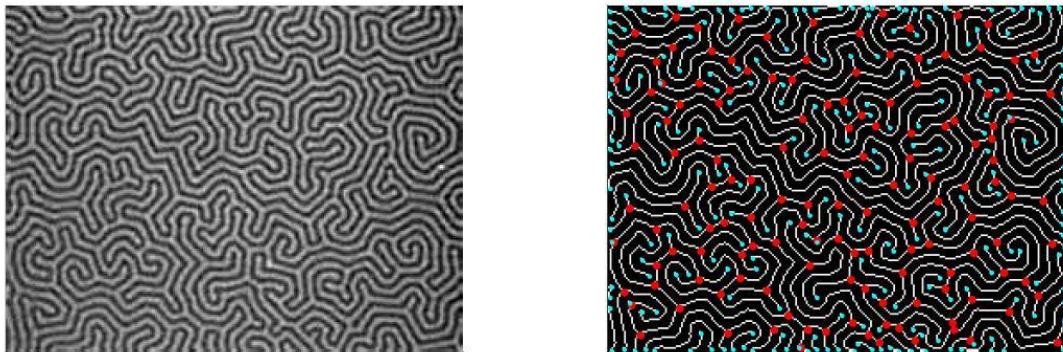


Fig.1. Left panel – magneto-optical halftone image of magnetic domain structure in a YIG thin film (Wang, Shang, Wu, Yang and Ji, Chin. Phys. Lett., vol. 33, 047502 (2016)). Right panel – a skeleton of the image (white lines), branching points (red dots), and end points (cyan dots) prepared using built-in Matlab functions [1].

This work was financially supported by the Ministry of Science and Higher Education of the Russian Federation (no. 075-15-2024-632).

Bibliography

- [1] R. C. Gonzalez, R. E. Woods and S. L. Eddins, Digital Image Processing Using MATLAB. 2nd ed., Tata McGraw Hill Education Private Limited. New Delhi (2010).
- [2] A. Vagov, S. Köstler, T. T. Saraiva, A. Yu. Aladyshkin, D. Y. Roditchev, A. A. Shanenko, and V. S. Stolyarov, unpublished.

Rare Earth-Doped Crystals for Quantum Network Applications

Yuhui Chen

School of Physics, Beijing Institute of Technology, Beijing 100081, China

Email: Stephen.chen@bit.edu.cn

Abstract:

Like the internet we currently have, a quantum network that connects multiple quantum nodes together can enable advanced applications such as distributed quantum computing. In this lecture, I will first discuss the six stages of a full quantum network, which can also be classified into three main stages that are the stages of pre-quantum network, prototype quantum network and advanced quantum network. Through the discussion on quantum internet, the importance of building a quantum memory and a quantum transducer between light and microwave will be unfolded. I will then talk about the requirements of building quantum memories and transducers, why the properties of rare earth doped crystals are suitable for this purpose, and some recent research outcomes.

Proximity effect in superconductor/magnet heterostructures

I.V. Bobkova

¹Moscow Institute of Physics and Technology, Dolgoprudny, Russia
email: ivbobkova@mail.ru

The lecture is devoted to fundamentals of proximity physics at interfaces of different materials. In general, the proximity effects are nanoscale-penetration of electronic correlations from one material to another. We begin with basic physics of proximity effects at superconductor/normal metal interfaces. Then interfaces between superconductors and magnets, such as metallic and insulating ferromagnets and antiferromagnets, are discussed. Experimental manifestations and applications of the proximity effects are considered. Recently, study of proximity effects has become increasingly relevant due to the discovery of 2D materials, which opens up unprecedented opportunities to design new materials with specified properties. In thin-film or a few layer van der Waals heterostructures the proximity regions occupy the entire system. For this reason, in many cases the guiding design principle is based on one or another proximity effect, which makes the study of proximity effects extremely important and timely.

Electrodynamic properties of superconductors: fundamentals and experimental approaches

B.Gorshunov

Moscow institute of physics and technology (national research university), Dolgoprudny,
Russia

email: bpgorshunov@gmail.com

Abstract

The most prominent features of a superconductor compared to a regular conductor/metal are the infinitesimal direct current (dc, i.e., at zero frequency, $\nu=0$) resistivity, $\rho_{dc}=0$, the presence of an energy gap in the density of states, and the Meissner effect. The first two lead to drastic transformations of the spectra of optical conductivity $\sigma_{opt}(\nu)$ and permittivity $\epsilon'(\nu)$ of a material when the temperature is lowered below the superconducting transition temperature T_c . The dc resistivity is represented in the spectrum of optical conductivity by a delta function, $\sigma_{opt}(\nu)=1/\rho_{dc}=A\delta(0)$; here A is the spectral weight of the delta function, which can be expressed in terms of the plasma frequency of the Cooper pairs superconducting condensate, $\nu_{pl}^{SC} = \frac{ne^2}{\pi m}$ (n , e and m are concentration, charge and mass, respectively, of the electrons which are involved in the formation of Cooper pairs)

respectively, of the electrons which are involved in the formation of Cooper pairs). The Kramers-Kronig relationships, which are based on the general causality principle, provide the “dielectric image” of this zero-frequency delta function, $\epsilon'(\nu) = -\left(\frac{\nu_{pl}^{SC}}{\nu}\right)^2$.

Measuring the temperature-dependent dielectric function $\epsilon'(\nu, T)$ of a superconductor provides with a unique opportunity to determine its fundamental characteristics, and thus to gain insight into the microscopic mechanisms behind the phenomenon. Optical spectroscopy allows to determine another fundamental characteristic of a superconductor, the energy gap Δ in the density of state, which is detected in the optical conductivity spectrum in the form of a sharp feature indicating breaking of the Cooper pairs by the electromagnetic quantum with the energy $h\nu \geq 2\Delta$ (h is the Planck's constant). A number of other specific electrodynamic properties of conventional low-temperature superconductors, and of high-temperature superconductors will be discussed, and some examples of spectroscopic studies performed at the MIPT Laboratory of terahertz spectroscopy on various superconducting compounds will be shown.

Theoretical study of flat band models and materials

Wei Jiang

School of Physics, Beijing Institute of Technology, Beijing 100081, China

Email: wjiang@bit.edu.cn

Abstract:

Lieb lattice has been extensively studied to realize ferromagnetism due to its exotic flat band. However, its material realization has remained elusive; so far only artificial Lieb lattices have been made experimentally. Here, based on first-principles and tight-binding calculations, we discover that a recently synthesized two-dimensional sp^2 carbon-conjugated covalent-organic framework (sp^2c -COF) represents a material realization of a Lieb-like lattice. The observed ferromagnetism upon doping arises from a Dirac (valence) band in a non-ideal Lieb lattice with strong electronic inhomogeneity (EI) rather than the topological flat band in an ideal Lieb lattice. The EI, as characterized with a large on-site energy difference and a strong dimerization interaction between the corner and edge-center ligands, quenches the kinetic energy of the usual dispersive Dirac band, subjecting to an instability against spin polarization. We predict an even higher spin density for monolayer sp^2c -COF to accommodate a higher doping concentration with reduced interlayer interaction.

Enhanced Study on the Utilization of Trace Gas Sensors for Early Disease Detection

Yangyang Ju

Abstract : Trace gas sensor technology holds significant potential for application in early disease detection due to its non-invasive, rapid, and convenient characteristics. As the importance of early disease detection in improving survival rates and reducing treatment costs becomes increasingly evident, trace gas sensors have emerged as a highly regarded diagnostic tool. By analyzing trace chemical components in exhaled breath, these sensors can identify biomarkers associated with specific diseases, providing a reliable basis for early screening. Currently, research on trace gas sensors has made remarkable progress. The development of high-sensitivity sensors, the integration of multi-parameter analysis detection systems, and the widespread adoption of portable real-time monitoring devices have enabled this technology to show great promise in the early diagnosis of diseases such as lung cancer, gastric cancer, and diabetes. Moreover, the incorporation of artificial intelligence and machine learning has further enhanced diagnostic accuracy and efficiency. We will explore the current state of applications, technological advancements, and future trends of trace gas sensors in early disease detection.

Insights into Soft Matter Dynamics and Structure via Three Entropic Effects

Peng Liu

In this talk, I explore the relationship between dynamics and structure in soft matter systems through three intriguing entropic effects. First, we discovered that lattice fluctuations can induce an attraction between colloidal particles carrying the same charge, challenging the conventional principle of "like charges repel, opposite charges attract." Using simulations and experiments, we introduced a new form of entropic force, where large particle lattice deformations generate effective attraction for smaller particles. Second, we studied entropy effects in active soft matter, finding that the strength of constraints in an active bath significantly shifts the entropic force from strong attraction to strong repulsion. Lastly, we examined the impact of compressibility on collective motion in chiral active matter. Through simulations and experiments, we observed spatial oscillations in boundary flow, tightly linked to the system's density distribution. These studies reveal the broad applications of entropy-driven effects in soft matter and the complexity of collective behavior.

Superconducting spintronics: interplay between superconductivity and magnetism

A. S. Mel'nikov^{1,2} *

¹ Moscow Institute of Physics and Technology (National Research University), Dolgoprudnyi, Moscow region 141701, Russia

² Institute for Physics of Microstructures, Russian Academy of Sciences, 603950 Nizhny Novgorod, GSP-105, Russia

*email: melnikov@ipmras.ru

Abstract

In this lecture I will give a review of basic physics underlying the modern works on superconducting spintronics. In particular, we will discuss the mechanisms of interaction of the magnetic and superconducting orderings and possible applications of these mechanisms in different cryoelectronic devices. The review will also include the discussion of the electrodynamic response of superconductor-ferromagnet (SF) and superconductor – normal metal (SN) hybrid structures: (i) electromagnetic proximity effect; (ii) inhomogeneous Fulde-Ferrel-Larkin-Ovchinnikov (FFLO) states in SF multilayers with the order parameter modulation in the plane of the layers; (iii) the effect of the Rashba – type spin-orbit (SO) coupling; (iv) paramagnetic Meissner effect in SN systems originated from the spin-triplet interlayer pairing.

We will also discuss modern approaches aimed to the tuning the symmetry of superconducting correlations in hybrid structures with proximity effect including the engineering of superconducting states with nontrivial topology.

Brain like artificial neural networks based on superconducting elements

Sidorenko¹, * A.S.

¹ Moscow Institute of Physics and Technology, Dolgoprudnyi, Russia

*email: anatolie.sidorenko@mib.utm.md

Abstract

Energy efficiency and the radically reduction of the power consumption level becomes a crucial parameter constraining the advance of supercomputers. The most promising solution is design and development of the non-von Neumann architectures, first of all – the Artificial Neural Networks (ANN) based on superconducting elements. Superconducting ANN needs elaboration of two main elements – nonlinear switch element [1] (neuron's core structure - S/F/S Josephson Junction is shown in Fig.1), and linear connecting element synapse [2]. We present results of our design and investigation of superconducting spin-valves and superconducting synapse, based on layered hybrid structures superconductor-ferromagnet.

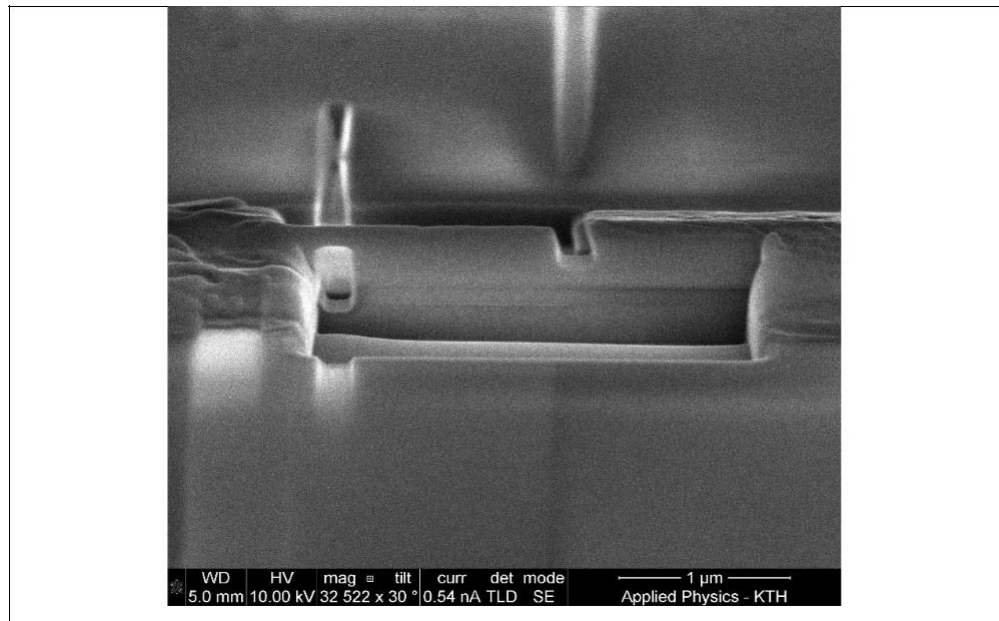


Fig.1 S/F/S Josephson junction – base element of the superconducting Gauss neuron

Bibliography

[1] Andrey E. Schegolev, Nikolay V. Klenov, Sergey V. Bakurskiy, Igor I. Soloviev, Mikhail Yu. Kupriyanov, Maxim V. Tereshonok and Anatoli S. Sidorenko. *Beilstein J. Nanotechnol.* 13, 444 (2022).

[2] S.Bakurskiy, M.Kupriyanov, N.Klenov, I.Soloviev, A.Schegolev, R.Morari, Yu.Khaydukov, A.Sidorenko. *Beilstein J. Nanotechnol.* 11, 1336 (2020).

Characterization of topological insulators and related materials using synchrotron radiation

Lada V. Yashina

Lomonosov Moscow State University, MIPT

*email: yashina@inorg.chem.msu.ru

Topological insulators are promising materials for future spintronic applications because they behave as bulk insulators and surface conductors simultaneously. Their metallic surface hosts Dirac-cone spin-polarized topological surface states that can be used as channels in which to drive pure spin currents or spin-polarized electrical currents on ultrafast time scales.

Topological insulators are studied in a form of complex single crystals or epitaxial films for which the following information should be precisely known and controlled: crystal structure including atomic position occupancy, elemental composition including component distribution along the crystal at different scales and surface composition, defect composition and dimensional defect density, i.e. crystal and surface perfection, electronic band structure and its variation on composition. Advance methods of characterization such as synchrotron-based ARPES, XPS, photoelectron diffraction, photoemission spectromicroscopy, HAADF STEM/EDX, STM/STS are discussed in this lecture.

Characterization and Manipulation of Intervalley Scattering in Graphene

Yu Zhang

Advanced Research Institute of Multidisciplinary Sciences, Beijing Institute of Technology,

Beijing 100081, China

Email: yzhang@bit.edu.cn

Intervalley scattering involves microscopic processes that electrons are scattered by atomic-scale defects on the nanoscale. Although central to our understanding of electronic properties of materials, direct characterization and manipulation of range and strength of the intervalley scattering induced by an individual atomic defect have so far been elusive. Using scanning tunneling microscope, we visualize and control the electronic properties especially the intervalley scattering from an individual monovacancy in graphene [1-3]. By directly imaging the affected range of monovacancy-induced intervalley scattering, we demonstrate that it is inversely proportional to the energy; i.e., it is proportional to the wavelength of massless Dirac fermions. A giant electron-hole asymmetry of the intervalley scattering is observed because the monovacancy is charged. By further charging the monovacancy, the bended electronic potential around the monovacancy softens the scattering potential, which, consequently, suppresses the intervalley scattering of the monovacancy [4].

References

- [1] Yu Zhang, et al. Phys. Rev. Lett. (2020) 125, 116804.
- [2] Yu Zhang, et al. Phys. Rev. B (2020) 101, 155424.
- [3] Yu Zhang, et al. Nano Lett. (2021) 21, 2526-2531.
- [4] Yu Zhang, et al. Phys. Rev. Lett. (2022) 129, 096402.

Controllable Construction and Electronic Properties Investigation of Low-Dimensional Materials by SPM

Quanzhen Zhang

School of Integrated Circuits and Electronics, Beijing, China

*email: quanzhen.zhang@bit.edu.cn

Abstract

Two-dimensional (2D) materials have drawn intensive attention since they can be manipulated to form different electronic structures, which gives rise to a variety of strongly correlated physical properties, once the long-range Coulomb interaction exceeds kinetic energy of electrons. Moreover, the construction of low-dimensional homostructures and heterostructures based on 2D transition-metal dichalcogenides (TMDs) has attracted widespread attention recently. Among them, the in-plane one-dimensional (1D) structures that consist of atomically thin TMDs with strongly correlated electrons are especially important, since they hold potential for exploring low dimensional correlated electronic properties.

Here we demonstrate that, using STM manipulation technique, we can precisely construct the 2D TMDs homojunctions and heterojunction based on the 2D atomic crystal thin T-NbSe₂ and H-NbSe₂ films, which provides a dynamic way to modify the correlated electronic states at the junctions. In the homojunction, we confirm the existence of 1D-confined potential at the homojunction of two single-layer 1T-NbSe₂ islands. Such potential is structurally sensitive, and shows a non-monotonic function of their interspacing. In the heterojunction, the H-NbSe₂ metallic state penetrates the Mott insulating T-NbSe₂ at the H/T phase interface, with a prominent 2D charge density wave (CDW) proximity effect. Moreover, an insulating Mott gap collapse with the disappearance of the upper Hubbard band is detected at the electronic phase transition region.

POSTERS

Spin supercurrent in superconductor/ferromagnet van-der-Waals heterostructures

G. A. Bobkov^{1*}, I. V. Bobkova¹, A. M. Bobkov¹
1 Moscow Institute of Physics and Technology, Dolgoprudny,
Russia *email: gabobkov@mail.ru

We study dissipationless spin transport induced by a charge supercurrent in a monolayer van der Waals superconductor under the applied magnetic field and in a bilayer superconductor/ferromagnet (S/F) heterostructure with no external field [1]. It is shown that in both cases a combined action of the Ising-type spin-orbit coupling and the Zeeman field results in appearance of a nonunitary superconducting triplet correlations with nonzero average Cooper pair spin, which carry spin current in the presence of a condensate motion. Properties of this dissipationless spin current are investigated. In particular, it is shown that it manifests a rectification effect. In addition, in S/F heterostructures the amplitude and the sign of the spin current are controlled by gating.

The work was supported by Grant from the ministry of science and higher education of the Russian Federation No. 075-15-2024-632

Bibliography

[1] G.A. Bobkov et. al arXiv:2407.01319

2D Edge Dependent local exciton on MoS₂

Weikang Dong^{1#}, Han Lin^{2*}, Jiafang Li^{1*}

¹ Key Lab of Advanced Optoelectronic Quantum Architecture and Measurement (Ministry of Education), Beijing Key Lab of Nanophotonics & Ultrafine Optoelectronic Systems, and School of Physics, Beijing Institute of Technology, Beijing 100081, China

²School of Science, RMIT University, Melbourne VIC 3000, Australia *email: jiafangli@bit.edu.cn, han.lin2@rmit.edu.au

Transition metal dichalcogenides (TMDCs) exhibit fascinating physics and have garnered significant attention due to their tunable exciton. Although recent advancements in edge-dependent exciton have been reported, achieving exciton tuning by different Mo/S ratios on edge remains a challenge. In this work, we successfully fabricate different Mo/S ratio edge structures on MoS₂, including circular (messy Mo/S ratio) and triangular (Mo/S = 4:1, 2:1, 1:1, 1:2, and 1:4) edges, using a Si₃N₄-protected focused ion beam (FIB) system. We demonstrate on triangle edge, a local exciton that experiences a redshift from the pristine 1.8 eV to 1.7 eV due to the high-order atomic arrangement, and exciton on the circle edge, present a blue shift to 1.9 eV, attributed to lower connection energy. Specifically, the exciton of triangular edge shows a significant intensity variation dependent on the Mo/S ratio, which the edge of Mo/S = 1: 4 present high intensity than other ratios. Furthermore, we find the triangular edge MoS₂ devices exhibit enhanced photocurrent on-off switching behavior using a time-resolved photodetector. These findings open a new way to tuning exciton by designing edge structures, which increases the field of photoelectric device applications.

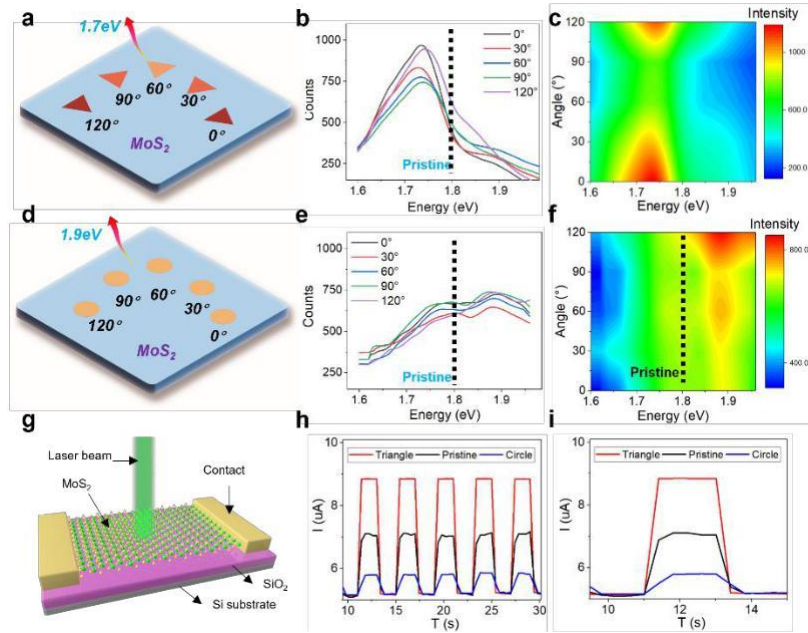


Figure. Edge angle and its PL properties. a) the schematic of triangle edge structure of 0, 30, 60, 90, and 120 degrees on MoS₂, the color of triangle present the intensity of 1.7 eV. b) the PL intensity of 0, 30, 60, 90, and 120 degrees, the black dashed line shows the pristine signal of 1.8 eV. c) the intensity mapping of 0, 30, 60, 90, and 120 degrees corresponding to b). d) the schematic of circle edge structure of 0, 30, 60, 90, and 120 degrees on MoS₂, the color of triangle present the intensity of 1.9 eV. e) the PL intensity of 0, 30, 60, 90, and 120 degrees, the black dashed line shows the pristine signal of 1.8 eV. f) the intensity mapping of 0, 30, 60, 90, and 120 degrees corresponding to e). g) the schematic of the device. h) Photocurrent on-off switching behavior in the MoS₂ device triangle-fabricated (red), circle-fabricated (blue), and with pristine (black). i) the photocurrent generation (τ_{rise}) and decay (τ_{decay}) times corresponding to h).

Bibliography

- [1] Z. Dai, G. Hu, Q. Ou. et al. Chem Rev, 120, 6197 (2020)
- [2] Z. Huang, W. Deng, Z. Zhang. et al, Advanced Materials, 35, 2211252 (2023)

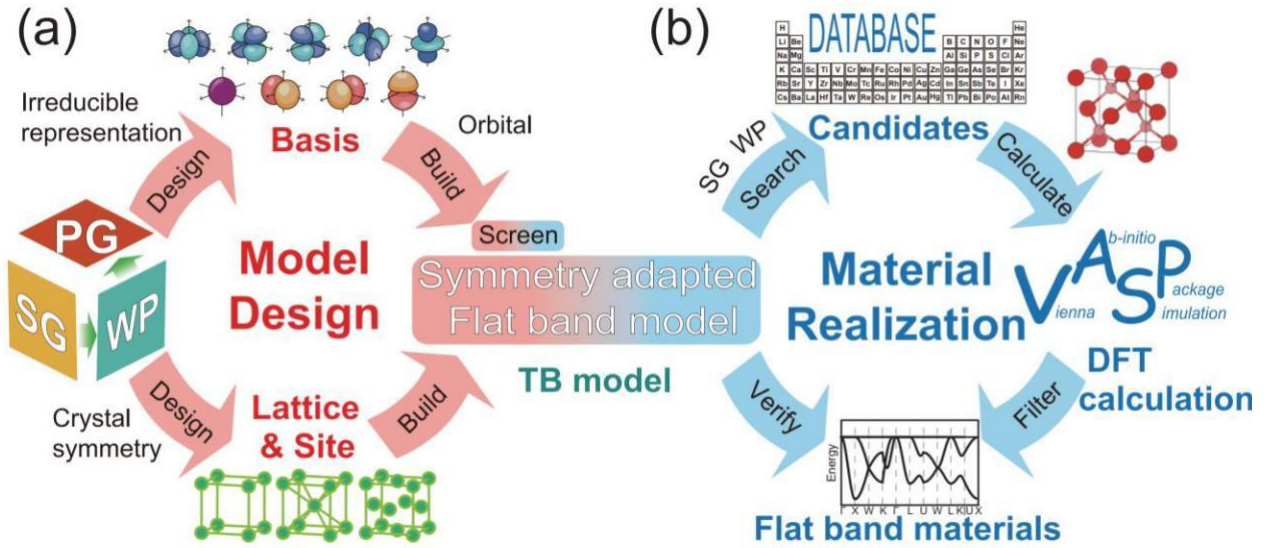
Three-Dimensional Multi-Orbital Flat Band Models and Materials

Jingyi Duan, Chaoxi Cui, Minjun Wang, Wei Jiang,* and Yugui Yao*

Centre for Quantum Physics, Key Laboratory of Advanced Optoelectronic Quantum Architecture and Measurement (MOE), School of Physics, Beijing Institute of Technology, Beijing 100081, China

*email: wjiang@bit.edu.cn & ygyao@bit.edu.cn

The study of flat band (FB) models and their physical manifestations serve as a crucial basis for probing exotic quantum phenomena associated with strong correlation. Here we present a systematic theoretical framework that simultaneously enable the construction of multi-orbital FB models and identification of feasible material candidates. This is achieved by integrating group theory and crystallography for the symmetry-adapted tight-binding model, which incorporate lattice, site, and orbital degrees of freedom. We elucidate this framework's practical applicability by uncovering a novel three-dimensional (3D) multi-orbital FB model in the basic face-centered cubic lattice, fundamentally distinct from typically studied single-orbital Lieb and Kagome models. Most importantly, we successfully identify a plethora of high-quality binary material candidates exhibiting ultra-clean 3D FB near the Fermi level. We further show the diversity of orbital bases within the model and expand our analysis to other cubic lattices with varying space groups for the realization of various 3D multi-orbital FB systems. We believe that this research lays a solid foundation for studying the correlated physics of FB systems, especially for multi-orbital systems.



Pic. 1 *Theoretical framework for exploring multi-orbital FB systems.* The FB searching framework contains two modules. (a) The first module handles the FB model design based on symmetry-adapted TB model designing, building, and screening processes, which consider the lattice, site, and orbital degrees of freedom. SG, PG, and WP represent the space group, point group, and Wyckoff position, respectively. (b) The second module handles the material realization by treating the FB materials searching, calculating, filtering and verification processes. It searches material candidates using the WP and SG information from the model design process, followed by high-throughput DFT calculations, and FB material verification.

Magnetic properties of the $\text{Mn}_{3-x}\text{Ni}_x\text{BO}_5$ Single Crystal

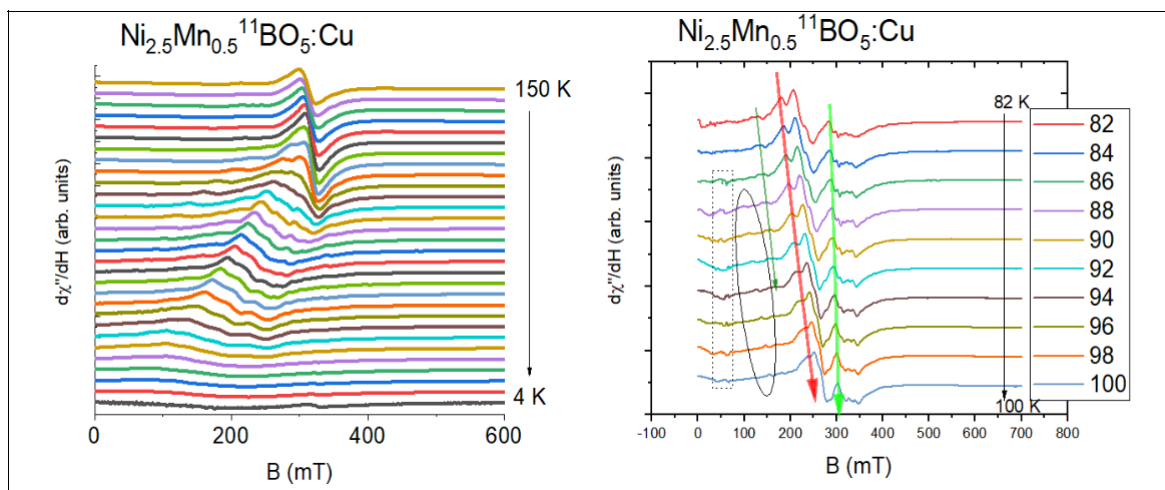
R.M. Eremina^{1,*}, E.M. Moshkina², I.V. Yatsyk³

¹ Zavoisky Physical-Technical Institute, FRC Kazan Scientific Center of RAS, Kazan, Russia

² Federal Research Center "Krasnoyarsk Science Center of the Siberian Branch of the Russian Academy of Sciences", Krasnoyarsk, Russia

*email: REremina@yandex.ru

Ludwigites are oxyborates with structural formula $(\text{M}^{2+})_2(\text{M}^{3+})\text{BO}_5$ with (M^{2+}) and (M^{3+}) stand for divalent and trivalent metals, respectively. The magnetic ions occupy four inequivalent positions in distorted octahedral coordination, which form edge-sharing zigzag walls perpendicular to the b axis. This leads to multiple unusual magnetic properties, observed in ludwigites. However, such ion distribution causes magnetic anisotropy in monocrystal structures. Some ludwigites exhibit negative magnetization values in magnetization-temperature relation measurements. $\text{Mn}_{3-x}\text{Ni}_x\text{BO}_5$ ($x = 0.5, 1.8$) compounds are shown to have this effect under Neel temperature of 81K and 92K at field value of 0.5 kOe, respectively [1]. Another compound with negative magnetization is $\text{Ni}_{5.33}\text{Ta}_{0.67}\text{B}_2\text{O}_{10}$ [2]. In this ludwigite magnetization in field cooling mode with $H=200$ Oe becomes negative at $T=30\text{K}$ – much lower, than Neel temperature of 165 K. In this work we present the results of the ESR studies on $\text{Mn}_{3-x}\text{Ni}_x\text{BO}_5$ monocrystal ludwigite. Single crystals oxyborate have been synthesized using flux crystal growth.



Pic.1 ESR spectra in $\text{Ni}_{2.5}\text{Mn}_{0.5}^{11}\text{BO}_5\text{:Cu}$ in X-band

The ESR spectra was obtained ($0 \leq B \leq 1.4$ T; $5 \leq T \leq 300$ K) using EMXplus (Bruker). From analysis of the temperature dependencies resonance field of ESR lines temperature dynamic processes were estimated. The number of ESR lines shown that ESR lines observed from Ni, Cu and Mn ions with strong temperature dependencies. (Pic. 1).

This research was supported by the Russian Science Foundation (project no. 23-72-00047).

Bibliography

- [1] L.N.Bezmaternykh, E.M.Kolesnikova, E.V.Eremin, S.N.Sofronova, N.V. Volkov, M.S. Molokeev, JMMM 364, 55-59, (2014).
- [2] S.N. Sofronova, N.V. Kazak, E.V. Eremin, E.M. Moshkina, A.V. Chernyshov, A.F. Bovina, Journal of Alloys and Compounds, 864, 158200 (2021).

Magnon-photon coupling in superconductor/ferromagnet heterostructures

V. M. Gordeeva^{1,*}, I. V. Bobkova¹, A. M. Bobkov¹, M. A. Silaev^{2,1}
Moscow Institute of Physics and Technology, Dolgoprudny, Russia
²Tampere University, Tampere, Finland
*email: gordeeva.vm@phystech.edu

Superconducting nanostructures with ferromagnetic interlayers are objects of interest to observe magnon-polariton modes with ultrastrong coupling between Kittel magnon and Swihart photon modes, which makes such structures promising for magnonics applications. In particular, it was shown experimentally [1] and theoretically [2] that ultrastrong magnon-photon coupling can be realized in S/F/S systems with an insulating ferromagnet and S/F/I/S systems with a metallic ferromagnet. Besides, it was recently demonstrated [3] that magnon-photon coupling in S/F/S structures with an insulating ferromagnet is strongly anisotropic due to the chirality of the dipolar stray field, which makes it possible to control the coupling strength by changing the direction of the saturation magnetization.

In the current work we theoretically describe magnon-photon coupling in S/F/I/F/S heterostructures with two metallic ferromagnets. It is demonstrated that the interaction between magnons in two ferromagnets carried by the Meissner currents in superconductors leads to giant splitting of the magnon-polariton modes, which corresponds to the ultrastrong coupling regime.

The work was supported by RSF project №22-42-04408.

Bibliography

- [1] I. A. Golovchanskiy et al., Phys. Rev. Appl. 16, 034029 (2021).
- [2] Mikhail Silaev, Phys. Rev. B 107, L180503 (2023).
- [3] Zhuolun Qiu et al., arXiv:2407.21597 (2024).

Magnetic proximity effect in superconductor/ferromagnet van der Waals heterostructures: dependence on the number of superconducting monolayers

A.S. Ianovskaia¹, G. A. Bobkov¹, A. M. Bobkov¹, I.V. Bobkova.^{1,2}

¹*Moscow Institute of Physics and Technology, 141701, Dolgoprudny, Russia*

²*National Research University Higher School of Economics, 101000 Moscow, Russia*

Magnetic proximity effect is well-studied in the heterostructures with the large number of monoatomic layers. For example, if the S layer is proximitized by a thin-film metallic ferromagnet and the S/F interface is fully transparent, the effective exchange field in the S layer is $\hbar_{eff} = v_F d_F h / (v_S d_S + v_F d_F)$ [1]. In this case there will be classical suppression of the order parameter by an effective exchange field, induced in the superconductor by ferromagnet, and one can see a DOS with Zeeman splitting.

Considering van der Waals S/F heterostructures, the effects of hybridization of electronic spectra turn out to be important due to the low number of monoatomic layers. Consequently, the superconducting state of such structure appears to be greatly modified compared to the case of the thin-film heterostructure [2].

In this work we report how the behavior of the superconducting state depends on a change in the number of monolayers. We investigated the evolution of the behavior of the superconducting order parameter as a function of the exchange field of the ferromagnet and as a function of the chemical potential of the ferromagnet. It is shown that these dependencies have a highly non-monotonic character, which directly reflects the physical mechanism of the proximity effect in such systems. Moreover, the limiting form of the dependence of the order parameter on the exchange field for a large number of superconducting layers is discussed.

Spin splitting of the electronic LDOS is also investigated. Analogously to the behavior of the superconducting order parameter this splitting is strongly different from the well-known picture of Zeeman-split superconducting LDOS. This unusual spin splitting of the LDOS can be observed experimentally upon varying the gate potential applied to the F-layer. The behavior of the superconducting order parameter can also be obtained from the LDOS observed experimentally via scanning tunneling microscopy (STM) technique.

The work was supported by the Russian Science Foundation via the project No. 24-12-00152

[1] Bergeret, F. S. and Volkov, A. F. and Efetov, K. B., Phys. Rev. Lett., 2001

[2] G. A. Bobkov et al., 2024, <https://doi.org/10.48550/arXiv.2405.07575>

SnS-Andreev spectroscopy study of superconducting gap structure of NaFe_{1-x}Co_xAs compounds

A. D. Ilina^{1,2,*}, S.A. Kuzmichev^{3,1}, I.A. Nikitchenkov^{3,1},

I.V. Morozov³, A.I. Shilov¹, E.O. Rakhmanov^{3,1}, T.E. Kuzmicheva¹

¹ P.N. Lebedev Physical Institute of the Russian Academy of Sciences, Moscow, Russia

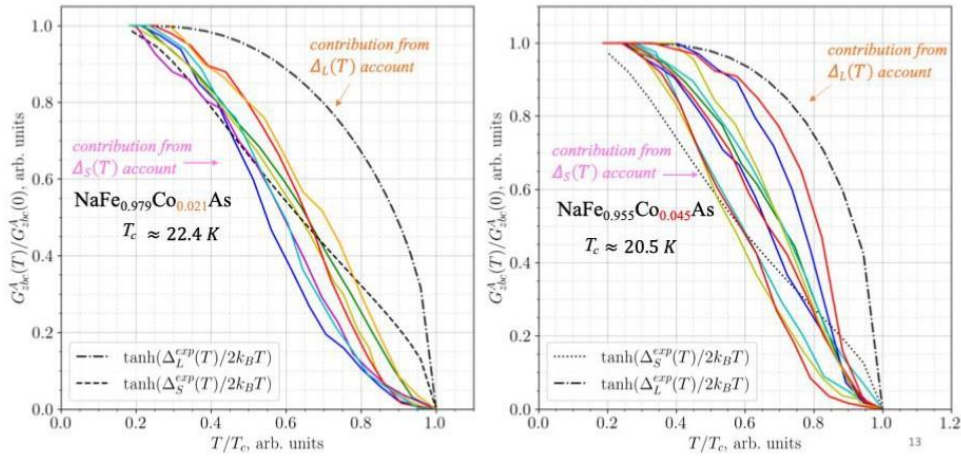
² Moscow Institute of Physics and Technology, Dolgoprudny, Russia ³

M. V. Lomonosov Moscow State University, Moscow, Russia

* anastasiailina2802@gmail.com

The layered iron-pnictide superconductor (SC) NaFe_{1-x}Co_xAs belongs to the 111 family and according to recent studies has anisotropic but nodeless SC gap structure. We used incoherent multiple Andreev reflection effect (IMARE) spectroscopy for two compositions with $x = 0.021$ ($T_c \approx 20.5$ K) and $x = 0.045$ ($T_c \approx 21.5$ K). Experimental “break-junction” technique [1] was used in order to create planar SnS-junctions (SC-thin normal metal-SC) where the IMARE occurs below T_c . IMARE shows an excess current in the $I(V)$ curve within the whole bias voltage range below T_c (as compared to $I(V)$ in the normal state), and an enhanced zero-bias conductance (ZBC) peak at $eV = 0$ in the dynamic conductance $dI(V)/dV$ spectrum [2]. According to [2], in a two-band approach the Andreev ZBC is $G_{Zbc}^A(T) = G(eV = 0) - G_N \propto \{(1 - \alpha) \tanh \frac{\Delta_L(T)}{2k_B T} + \alpha \tanh \frac{\Delta_S(T)}{2k_B T}\}$ (1) (G_N is the normal-state conductance of the junction, α is free parameter). As well, a series of $dI(V)/dV$ features called subharmonic gap structure [3] appears at positions $eV_n(T) = \frac{2\Delta(T)}{n}$, $n = 1, 2, \dots$

Here we observe a two-gap superconductivity of Na(Fe,Co)As and directly determined the magnitudes $\Delta_L(0)$ and $\Delta_S(0)$, characteristic ratios, and temperature dependences of the SC order parameters [4]. As well, for various ScS-junctions we collected the statistics on the Andreev ZBC temperature dependence (Pic. 1) and simulate it with formula (1) using experimental $\Delta_L(T)$ and $\Delta_S(T)$. The experimental data (solid lines) lay in between of the theoretical [2] partial band contributions (dash and dash-dot lines) within $T < T_c/2$. Significant reduction in the G_{Zbc}^A near T_c can be caused by the IMARE suppression at $eV \rightarrow 0$ due to inelastic scattering or low electron density of states at the Fermi energy.



Pic.1.

Bibliography

1. S.A. Kuzmichev, T.E. Kuzmicheva, Low Temp. Phys. **42**, 1008 (2016)
2. Günsenheimer U. , Zaikin A. D., Phys. Rev. B **50**(9), 6317 (1994)
3. R. Kümmel, U. Günsenheimer, R. Nicolsky, Phys. Rev. B **42**, 3992 (1990)
4. S.A. Kuzmichev, et al., JETP Lett. **120**, 125 (2024).

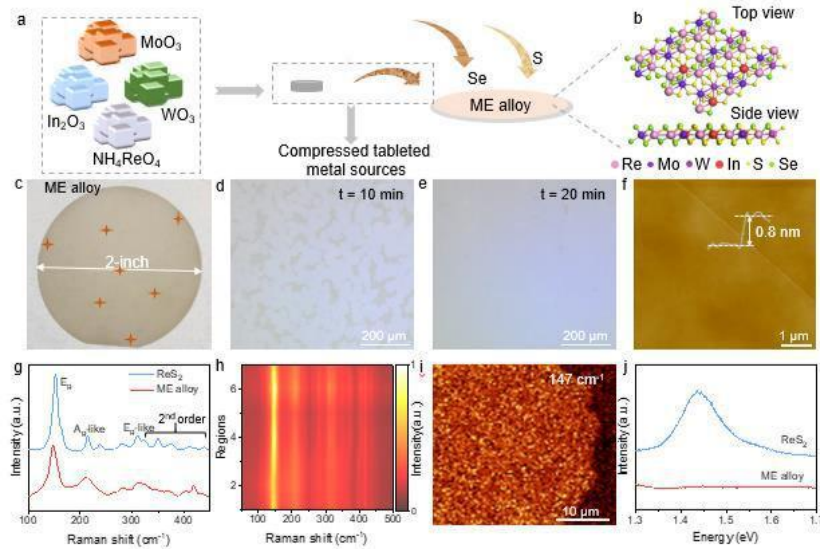
Mixing entropy engineering

Lin Jia, Ruichun Luo, Xiaoyu Zheng, Ping Wang, Lu Lv, Longyi Fu, Weikang Dong, Chunyu Zhao, Dian Li, Minghui Li, Jing Li, Yang Yang, Denan Kong, Jijian Liu, Qingmei Hu, Yang Zhao, Yan Xiong, Wu Zhou^{*}, Jiadong Zhou^{*}, Yao Zhou^{*}

Beijing Institute of Technology, Beijing, China

email: jialin@bit.edu.cn

Mixing entropy engineering is a promising strategy to tune the physical and chemical properties of materials. Although high-entropy in van der Waals bulk solids have been reported, entropy engineering in 2D monolayer remains unconquered. In this work, we report the epitaxial growth of 2-inch 1T'' hexanary medium-entropy alloy monolayers ($\text{Re}_a\text{W}_b\text{Mo}_c\text{In}_d\text{S}_x\text{Se}_y$) via chemical vapor deposition method. The atomic structure and chemical composition are confirmed by X-ray photoelectron spectroscopy, scanning transmission electron microscopy, energy dispersive X-ray spectroscopy and electron energy loss spectroscopy, illustrating the uniform distribution of the six elements. The hexanary medium-entropy alloy field-effect transistors exhibit metallic transport behavior and photodetectors show an ultrawide photo response from visible to near-infrared wavelengths with a responsivity of 110.2 A W^{-1} under 520 nm laser illumination. Meanwhile, the hexanary medium-entropy alloy monolayer exhibits excellent electrocatalytic hydrogen production with an overpotential of 176.6 mV in dark. Importantly, an overpotential of 43.7 mV at 10 mA cm^{-2} with a lowered Tafel slope of 51.9 mV dec^{-1} under 520 nm laser irradiation is obtained due to excellent electrical conductivity. Our work opens a new way to design mixing entropy alloys and realize the application of transition metal dichalcogenides (TMDs) in photo-enhanced electrocatalytic hydrogen production.



Research on Electrochemical Biosensors Based on Topological Materials

Yujiu Jiang^{1,2,3} Junfeng Han^{1,2,3,*}

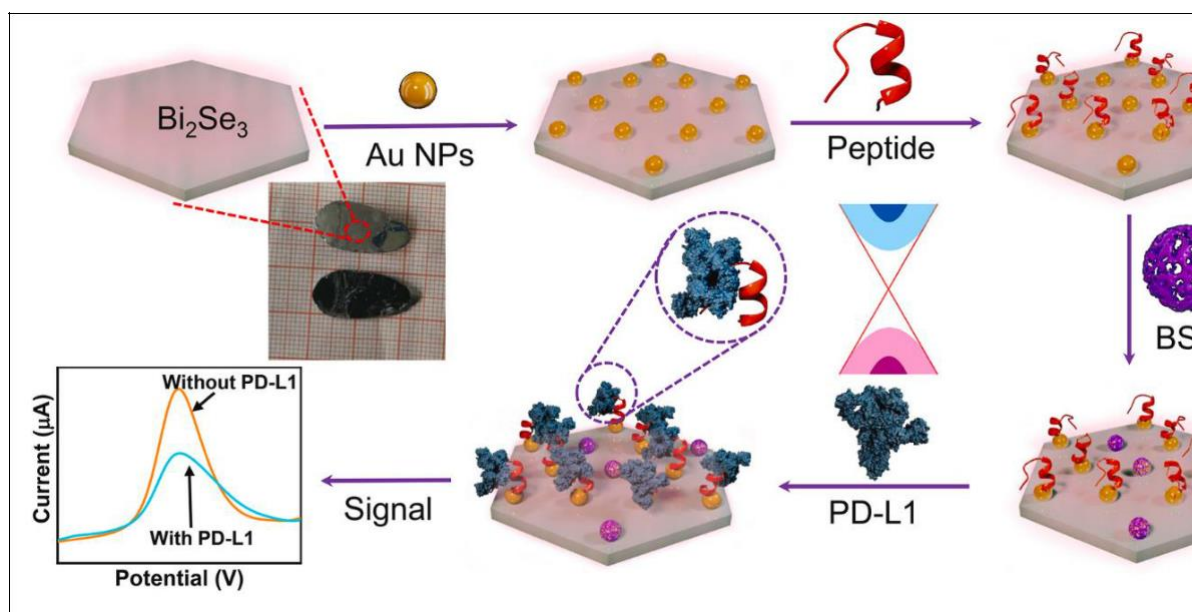
¹ Centre for Quantum Physics, Key Laboratory of Advanced Optoelectronic Quantum Architecture and Measurement (MOE), School of Physics, Beijing Institute of Technology, Beijing, 100081, China

² International Center for Quantum Materials, Beijing Institute of Technology, Zhuhai, 519000, China

³ Beijing Key Lab of Nanophotonics and Ultrafine Optoelectronic Systems, School of Physics, Beijing Institute of Technology, Beijing, 100081, China

*email: pkuhjf@bit.edu.cn

Topological materials are a new class of quantum materials, which have robust surface states with Dirac-like electronic structures. The robust surface state is originated from the intrinsic bulk properties and is immune to the defects and impurities. The use of the topological surface state in the solid-liquid interface for electrochemical detection avoids the interference from defects and impurities. Programmed cell death-1 (PD-L1) is an important immune checkpoint protein. PD-L1 expression has become a predictive biomarker of response to immune checkpoint inhibitors (ICIs) in several types of solid tumors. In this work, we developed a biosensor based on the topological insulator material Bi_2Se_3 with a targeting peptide on it. the biosensor based on topological insulator material with peptide on it has great potential in the application of detecting various biomarkers of diseases.



Pic.1

Bibliography

[1] Yujiu Jiang, Peng Zhu, Jinge Zhao, Shanshan Li, Yetong Wu, Xiaolu Xiong, Xu Zhang, Yuxiang Liu, Jiangyue Bai, Zihang Wang, Shiqi Xu, Minxuan Wang, Tinglu Song, Zhiwei Wang, Weizhi Wang, Junfeng Han, *Anal. Chim. Acta* 1239, 340655 (2023).

A Universal Strategy for Synthesis of 2D Ternary Transition Metal Phosphorous Chalcogenides

Yang Yang^{1#}, Jijian Liu^{1#}, Chunyu Zhao^{1#}, Jiadong Zhou^{1*}

¹Centre for Quantum Physics, Key Laboratory of Advanced Optoelectronic Quantum Architecture and Measurement (MOE), School of Physics, Beijing Institute of Technology, Beijing 100081, China *email: jdzhou@bit.edu.cn

The 2D ternary transition metal phosphorous chalcogenides (TMPCs) have attracted extensive research interest due to their widely tunable band gap, rich electronic properties, inherent magnetic and ferroelectric properties. However, the synthesis of TMPCs via chemical vapor deposition (CVD) is still challenging since it is difficult to control reactions among multi-precursors. Here, a subtractive element growth mechanism is proposed to controllably synthesize the TMPCs. Based on the growth mechanism, the TMPCs including FePS₃, FePSe₃, MnPS₃, MnPSe₃, CdPS₃, CdPSe₃, In₂P₃S₉, and SnPS₃ are achieved successfully and further confirmed by Raman, second-harmonic generation (SHG), and scanning transmission electron microscopy (STEM). The typical TMPCs–SnPS₃ shows a strong SHG signal at 1064 nm, with an effective nonlinear susceptibility $\chi^{(2)}$ of $8.41 \times 10^{-11} \text{ m V}^{-1}$, which is about 8 times of that in MoS₂. And the photodetector based on CdPSe₃ exhibits superior detection performances with responsivity of 582 mAW^{-1} , high detectivity of $3.19 \times 10^{11} \text{ Jones}$, and fast rise time of 611 μs , which is better than most previously reported TMPCs-based photodetectors. These results demonstrate the high quality of TMPCs and promote the exploration of the optical properties of 2D TMPCs for their applications in optoelectronics.

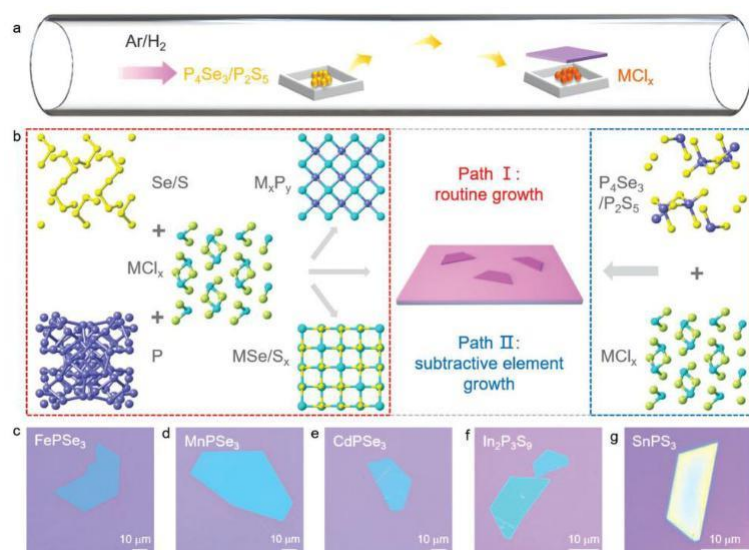


Figure 1. **a)** Schematic of the CVD process via subtractive-element-based growth strategy. **b)** The mechanism of routine and subtractive element growth. **c–g)** Optical images of the synthesized FePSe₃, MnPSe₃, CdPSe₃, In₂P₃S₉, and SnPS₃.

Bibliography

- [1] Y. Yang, J. Liu, C. Zhao, et al. Adv. Mater. 36, 2307237 (2024).
- [2] Zhou, J., Zhu, C., Zhou, Y. et al. Nat. Mater. 22, 450–458 (2023).

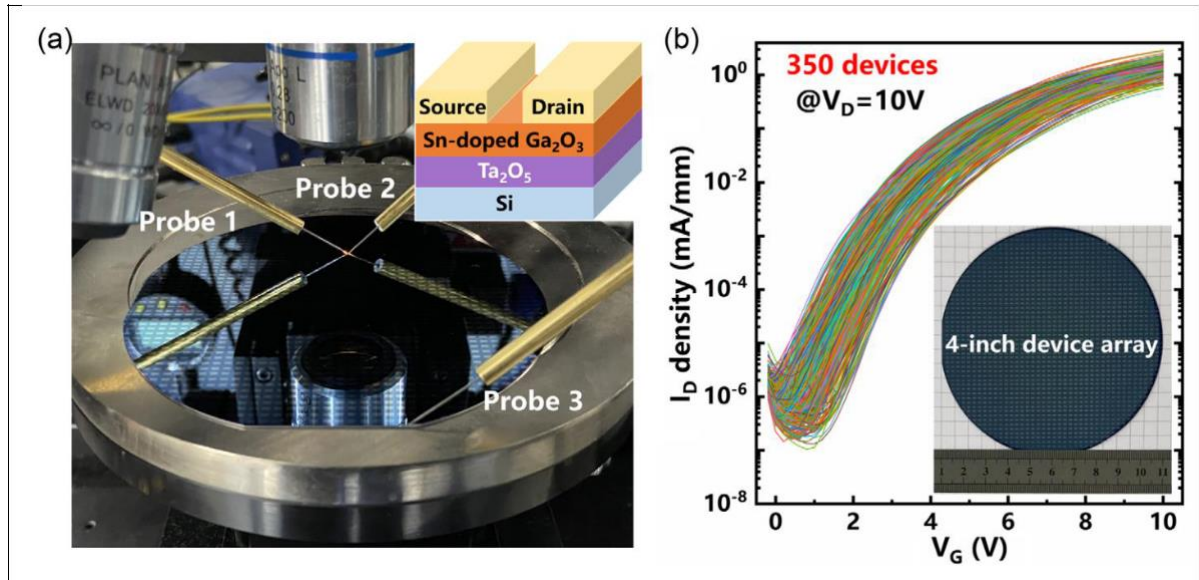
4 inch Gallium Oxide Field-Effect Transistors Array with High-k Ta₂O₅ as Gate Dielectric by Physical Vapor Deposition

Zi Chun Liu¹, Yuan Xiao Ma^{1,*}, Ye Liang Wang^{1,*}

¹ Beijing Institute of Technology, Beijing, China

*email: yxma@bit.edu.cn; yeliang.wang@bit.edu.cn

Field-effect transistors (FETs) with ultra-wide bandgap semiconductor Ga₂O₃ have been fabricated by physical vapor deposition with advantages of low cost, wafer scale, and rapid production. The insulator-like pristine Ga₂O₃ is converted to semiconductor by co-sputtering Sn with post-annealing, which demonstrates a 5.6×10^7 times higher on-state current. Importantly, this Sn-doped Ga₂O₃ sample shows a high breakdown voltage near 500 V. Furthermore, a 4 inch array of Sn-doped Ga₂O₃ FETs with high-k Ta₂O₅ gate dielectric has been fabricated on a silicon substrate, successfully showing a large on-current density of 1.3 mA mm^{-1} , a high $I_{\text{ON}}/I_{\text{OFF}}$ of 2.5×10^6 , and a low threshold voltage of 3.9 V, which are extracted from the average 350 devices. This work paves a promising way for Ga₂O₃-based nanoelectronics to serve medium-high voltage with low cost, rapid, and wafer-scale



production.

Fig.1 (a) The photo of the fabricated 4 inch device array during data measurement. (b) Transfer curves of 350 randomly-measured FETs. The inset in (b) shows the 4 inch device array.

The local electronic structure of the antiferromagnet CeCo₂P₂ exhibiting the Kondo effect

A. A. Minaev¹, * A. S. Frolov², V. S. Stolyarov¹

¹ Moscow Institute of Physics and Technology, 141700 Dolgoprudny, Russia
² Department of Chemistry, Moscow State University, Moscow, Russia
*email: minaev.aa@phystech.edu

Recently, special attention has been paid to 4f compounds, which are examples of strongly correlated systems where unusual bulk effects such as superconductivity, mixed valence, magnetism or the Kondo effect are realized. However, surface phenomena are no less interesting but poorly understood. Thus on the surface there can be reconstruction and relaxation, also the Kondo effect, which may not exist in the volume, and the local electronic structure behaves differently than in the depth of the material. An example of such materials is CeCo₂P₂, which exhibits a surface Kondo lattice formed by cerium atoms[1].

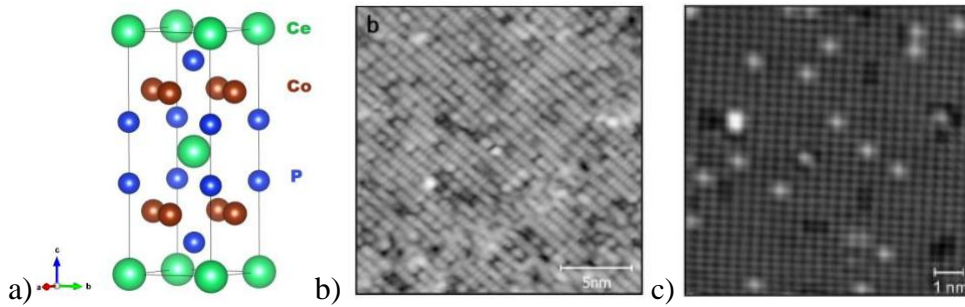
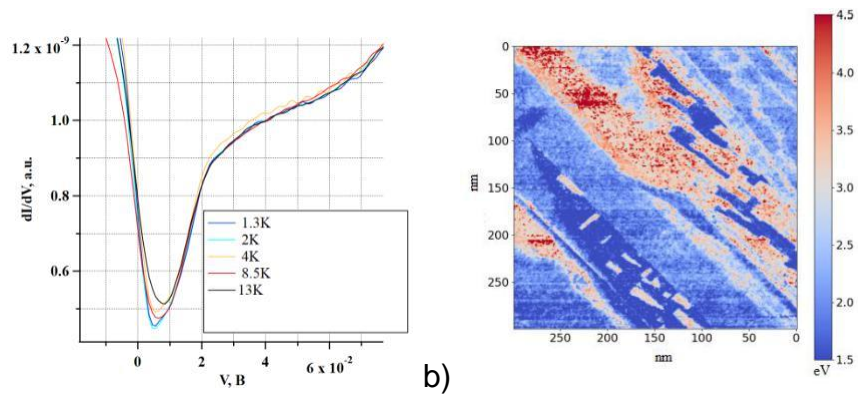


Fig.1 (a) Crystal structure CeCo₂P₂, topography of (b) Ce-termination, (c) P-termination

By applying scanning tunneling spectroscopy three fundamentally different terminations were found, with the cerium surface being a reconstructed 2×1 as shown in Fig. 1. Resonant field emission spectra in Fig. 2 were measured to determine the yield work of the different terminations. It is found that the surface terminated with cerium atoms exhibits a yield work of $\phi = (2.1 \pm 0.3)$ eV and phosphorus atoms $\phi = (3.8 \pm 0.3)$ eV. These values agree with known yield work values for elemental substances and can be used to identify surface terminations. It was found that there is a narrow dip near the Fermi level on the electronic state density spectra in Fig. 2, which decreases with increasing temperature from 1.4K to 13.8K on the cerium surface. And at 77K, this feature is not observed at all in the same voltage interval. That is, the obtained result indicates that the cerium lattice is a Kondo lattice.



(a) Density of states spectra of the cerium surface (b) Work function map of the CeCo2P2

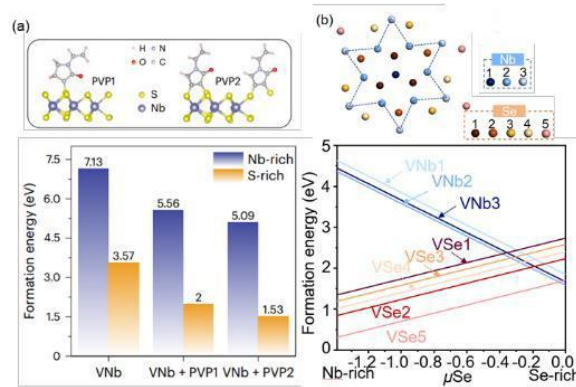
Bibliography

[1] G. Poelchen [et al.]. Interlayer Coupling of a Two-Dimensional Kondo Lattice with a Ferromagnetic Surface in the Antiferromagnet CeCo2P2 // ACS Nano. 2022. V. 16(3). P. 3573–3581.

Defect engineering in monolayer transition metal dichalcogenides

Mengmeng Niu^{1,*} Jingsi Qiao¹, Yeliang Wang¹
1 Beijing Institute of Technology, Beijing,
China *email: mengmniu@bit.edu.cn

Atomically precise defect engineering is an effective method to modulate the physical properties of transition metal dichalcogenides (TMD), making them promising candidates for various applications, including electronics, optoelectronics, and catalysis, etc. However, constructed precise vacancies, especially metal vacancies, are limited. The effect of defects on electron-correlated properties is poorly understood. Recently, precisely fabricating metal and chalcogen vacancies in TMD has been achieved by molecular modification.^[1] Besides, we investigated the properties of 1T-NbSe₂ charge density wave (CDW) monolayer with various single Se/Nb vacancy using density functional theory calculations.^[2] We found a unique Se vacancy site, called magic Se vacancy, could precisely erase the Mott electrons. Besides, Mott electrons could be more flexibly manipulated when the magic Se site is substituted with As, Br and K elements. The electronic properties of 1T-NbSe₂ with defects are tuned by the synergistic effect of compressive strain and electron doping. Our findings reveal that defect engineering is an ingenious strategy for atomically manipulating electron-correlated properties and manufacturing electronic patterns, guiding to erase and write in Mott



Pic.1. (a) Atomic models and formation energies of metal vacancy in pristine and PVP-capped 1H-NbS₂. (b) Eight types of vacancies in the Charge-Transfer insulator 1T-NbSe₂ supercell were considered.

electrons in two-dimensional materials.

Bibliography

- [1] Han, X., **Niu, M.**, Luo, Y. et al. *Nat. Synth* 3, 586-594 (2024).
- [2] **Niu M.**, Dai J, Qiao J. et al. To be submitted (2024).

Surface spin-flop in antiferromagnetic topological insulator $\text{Ge}_{0.4}\text{Mn}_{0.6}\text{Bi}_2\text{Te}_4$

E.V. Ponamarev^{12,*}, A.S. Frolov¹, D.Y. Usachov¹, V.S. Stolyarov¹²

¹Moscow Institute of Physics and Technology, Moscow,
Russia ²Dukhov automatics research institute, Moscow,
Russia *email: Ponamarev.ev@phystech.su

Topological insulators (TI) are a new class of materials that are interesting due to their properties and practical applications. The studied sample $\text{Ge}_{0.4}\text{Mn}_{0.6}\text{Bi}_2\text{Te}_4$ is an antiferromagnetic topological insulator with a layered change in magnetic moment (A-type order). The study is motivated by an interest in the surface-related magnetic properties of TI, which define the surface electronic structure. Using cryogenic magnetic force microscopy, magnetic signal maps were obtained in the field range $[-6.100, -2.025]$ T. Measurements for the positive and negative directions of the fields were carried out in different places of the sample. These studies show different behavior of domains with different directions of the magnetic moment of the first layer. The difference of signals on the domains (domain contrast) is shown in figure 1.a The data obtained show that the bulk spin flop (BSF) effect occurred at 2.3 T. We also see that the surface spin flop occurs at different fields for two types of domains: at 1.3 T for domains whose upper layer is directed against the field (SSFa), and at 1.9 T for those in which the upper layer is aligned with the external field (SSFp). The magnetic state with pronounced spatial fluctuations of magnetization was detected and has not been observed before. We studied the temperature dependence of magnetization in the range $T = 5.7\text{--}19.1\text{K}$, as well as at different distances from the magnetic probe to the sample: 50–150 nm. The Neel temperature for this sample was found to be 13 K and corresponds well to the value measured before [2]. The magnetic properties were modeled using quantum simulation within Heisenberg model. The field of the bulk spin-flop effect and saturation fields along various crystallographic axes and the Neel temperature were reproduced. It was also possible to qualitatively reproduce the surface SSFa spin-flop transition. The difference in the magnetization of the first layers depending on the field is shown in picture 1.b.

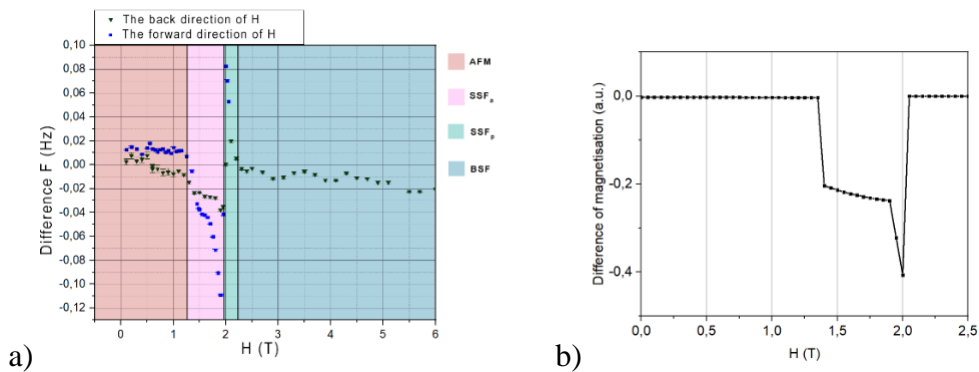


Fig.1 a) The dependence of the domain contrast on the magnetic field, measured using MFM b) Reproduced within Heisenberg model.

Bibliography

- [1] M.M. Otrokov, Nature 576(7787), 416-422 (2019).
- [2] A.S. Frolov, D.Y. Usachov, Commun. Phys. 7, 180 (2024).

Influence of capacitance and thermal fluctuations on the Josephson diode effect in asymmetric higher-harmonic SQUIDs

G. S. Seleznev^{1,2,*} and Ya. V. Fominov^{1,2,3}

¹ L. D. Landau Institute for Theoretical Physics RAS, Chernogolovka, Russia ²
Moscow Institute of Physics and Technology, Dolgoprudny, Russia

³ HSE University, Moscow, Russia

*email: seleznev.gs@phystech.edu

Asymmetric two-junction SQUIDs with different current-phase relations in the two Josephson junctions, involving higher Josephson harmonics, demonstrate a flux-tunable Josephson diode effect (asymmetry between currents flowing in the opposite directions, which can be tuned by the magnetic flux through the interferometer loop) [1,2]. We theoretically investigate influence of junction capacitance and thermal fluctuations on performance of such Josephson diodes. Our main focus is on the "minimal model" with one junction in the SQUID loop possessing the sinusoidal current-phase relation and the other one featuring additional second harmonic. Capacitance generally weakens the diode effect in the resistive branch (R state) of the current-voltage characteristic (CVC) both in the absence and in the presence of external ac irradiation. At the same time, it leads to qualitatively new features of the Josephson diode effect such as asymmetry of the retrapping currents (which are a manifestation of hysteretic CVC). In particular, the limiting case of the single-sided hysteresis becomes accessible. In its turn, thermal fluctuations are known to lead to nonzero average voltages at any finite current, even below the critical value [3]. We demonstrate that in the diode regime, the fluctuation-induced voltage can become strongly (exponentially) asymmetric. In addition, we find asymmetry of the switching currents arising both due to thermal activation and due to Josephson plasma resonances in the presence of ac irradiation.

Bibliography

- [1] Ya. V. Fominov and D. S. Mikhailov, Phys. Rev. B 106, 134514 (2022).
- [2] R. S. Souto, M. Leijnse, and C. Schrade, Phys. Rev. Lett. 129, 267702 (2022).
- [3] V. Ambegaokar and B. I. Halperin, Phys. Rev. Lett. 22, 1364 (1969).

Magnetic properties of the $(\text{Mg}_{1-x}\text{Ni}_x)_3\text{Si}_2\text{O}_5(\text{OH})_4$, $x = 2/3$ and 1

A.V. Shestakov^{1, *}, N.A. Belskaya², E.K. Khrapova², I.V. Yatsyk³,
I.I. Fazlizhanov³, R.G. Batulin⁴, R.M. Eremina³ and A.A. Krasilin²

¹Prokhorov General Physics Institute of the Russian Academy of Sciences, Moscow, Russia

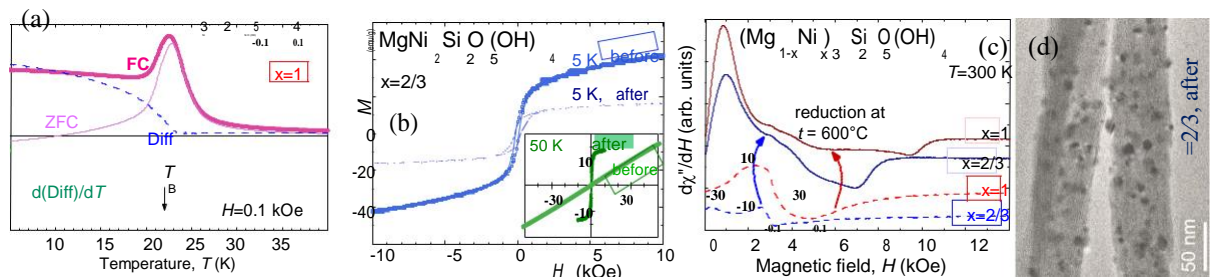
²Ioffe Institute, St.-Petersburg, Russia

³Zavoisky Physical-Technical Institute, FRC Kazan Scientific Center of RAS, Kazan, Russia

⁴Kazan Federal University, Kazan, Russia

*email: AlekseiVShestakov@gmail.com

The growing interest in the synthesis and modification of phyllosilicate (layered hydrosilicate) nanoparticles is due to the wide range of their applications [1, 2, 3, 4]. Only a few recent papers have reported magnetic properties of synthetic phyllosilicates doped with transition elements (Ni^{2+} ; Fe^{3+}) [5, 6]. In this work, $\text{Ni}_3\text{Si}_2\text{O}_5(\text{OH})_4$ and $\text{MgNi}_2\text{Si}_2\text{O}_5(\text{OH})_4$ were studied before and after reduction (in Ar- H_2 flow, 600 °C, 10 hours) using DC magnetometry and electron spin resonance (ESR) methods. The aim of the reduction was formation of metal Ni^0 -particles.



Pic.2(a) Determination of blocking temperature by FC-ZFC magnetization difference; (b) magnetization isotherms before & after reduction $x=2/3$; (c) ESR spectra; (d) TEM image for $x=2/3$.

The magnetization was obtained ($0 \leq B \leq 9$ T; $5 \leq T \leq 300$ K) using the PPMS-9 platform (Quantum Design, USA). From analysis of temperature dependencies of first derivative of differences of FC and ZFC magnetization temperature blocking T_B [7] (Pic. 2a). Constant C and temperature θ (from Curie-Weiss law) were estimated. The magnetization isomers after reduction exhibit superparamagnetic behavior (Pic. 2b). The ESR spectra was obtained ($0 \leq B \leq 1.4$ T; $5 \leq T \leq 715$ K) using EMXplus (Bruker) and Varian 12. From analysis of the temperature dependencies resonance field of ESR lines temperature Curie T_C was estimated. Before annealing, ESR lines from the Ni^{2+} ion in the paramagnetic state and additional lines from clusters are visible; after annealing, we see nickel particles in the superparamagnetic state. (Pic. 2c, d).

Bibliography

- [1] S. Ganguly, S. Margel, J. Compos. Sci. **6** (1), [15](#) (2022).
- [2] Y. Naciri, M. N. Ghazzal, E. Paineau, Adv. Colloid Interface Sci. **326**, [103139](#) (2024).
- [3] A.A. Krasilin, D.P. Danilovitch *et al.*, Appl. Clay Sci. **173**, [1–11](#) (2019).
- [4] Z. Bian, S. Kawi, Catal. Today **339**, [3–23](#) (2020).
- [5] E. Borghi, M. Occhiuzzi *et al.*, Phys. Chem. Chem. Phys. **12** (1) [227–238](#) (2009).
- [6] A. A. Krasilin, A. S. Semenova, *et al.*, Europhys. Lett. **113** (4) [47006](#) (2016).
- [7] I. J. Bruvera, P. Mendoza Zélis *et al.*, J. Appl. Phys. **118**, [184304](#) (2015).

0- π transition in planar Josephson S-N-S junction on a ferromagnetic insulator substrate

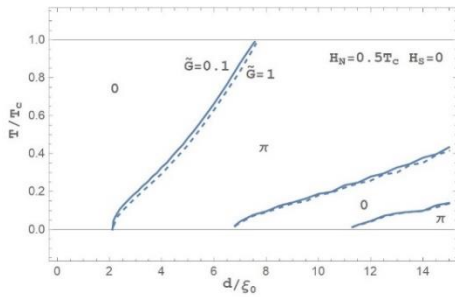
*E.A. Stadnik^{1,2}, K.B. Polevoy^{1,2}, I.V. Bobkova¹, A.M. Bobkov¹, V.S. Stolyarov^{1,2}, A.G. Shishkin^{1,2}

¹ Moscow Institute of Physics and Technology (MIPT), Dolgoprudny, Russia

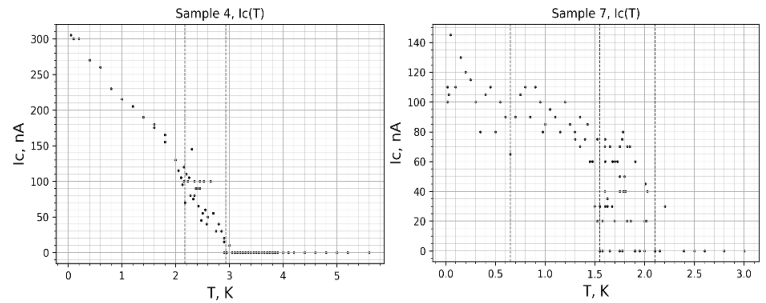
² NL Dukhov All-Russian Scientific Research Institute of Automation (VNIIA), Moscow, Russia

*email: Stadnik.EA@phystech.edu

The work is devoted to experimental investigation of a planar Josephson junction with normal metal barrier on a ferromagnetic insulator substrate. According to theoretical studies, conducted by A.M. Bobkov and I.V. Bobkova, such a system should, under certain conditions, undergo a transition from a 0-state to a π -state. More precisely – depending on a combination of material properties (coherence length of a normal metal, S-N interface transparency, metal resistance etc.) there are alternating regions of 0- and π -states on a phase diagram of such a contact.



Pic.1 – calculated phase diagram of a junction in (d, T) coordinates



Pic.2 – $I_c(T)$ dependences, obtained from measurements of two junctions

Several samples have been manufactured and measured at low temperatures, using BlueForce dilution refrigerator. IV measurements were conducted with a regular 4-probe scheme in a wide range of temperatures. Critical currents were determined by fitting IV characteristics and plotted against temperature – resulting $I_c(T)$ dependences are shown at Pic.2

$I_c(T)$ dependences have features, resembling those of a π -transition, while absolute values of I_c differ from those of a conventional SNS for more than an order of magnitude, which indicates the influence of FI on junction properties. Thus it has been shown that a ferromagnetic insulator substrate of micron thickness allows for a Josephson junction with measurable critical currents. Although current data does not provide unambiguous proof for a π -transition, further improvement will allow to observe the transition more reliably.

Bibliography

- [1] V. V. Ryazanov, V. A. Oboznov, Phys. Rev. Lett. 86, 2427 (2001).
- [2] A. V. Ustinov, V. K. Kaplunenko, Journal of Applied Physics 94, 5405 (2003).
- [3] T. E. Golikova et al, Supercond. Sci. Technol. 34 095001 (2021).

Synthesis and properties of materials based on mixed manganese, indium and bismuth tellurides

K.S. Strebko¹, * A.S. Frolov^{1,2}, A.I. Sergeev^{1,2}

¹ M. V. Lomonosov Moscow State University, Moscow, Russia

² Moscow Institute of Physics and Technology, Moscow, Russia

*email: kirills_str@mail.ru

Abstract

Topological insulators are materials that have band gap in bulk like semiconductors, but have electronic conductors on surface. MnBi_2Te_4 belongs to these class of such materials, and exhibits magnetic properties AFM. Such materials can be applied in the field of spintronics. Adding superconductivity to the properties of magnetic topological insulators will lead to using such materials in quantum computing devices, which can be achieved by doping MnBi_2Te_4 with indium. Thus, the purpose of this work is to synthesize and study the electronic properties of $\text{Mn}(\text{In}_x\text{Bi}_{1-x})_2\text{Te}_4$ compounds.

The synthesis of MnBi_4Te_7 and $\text{MnBi}_6\text{Te}_{10}$ crystals was performed using a modified Bridgman method. The samples obtained were diagnosed using X-ray fluorescence spectroscopy (XFS) and X-ray diffraction analysis (XRD). The analysis data confirmed that the compositions MnBi_4Te_7 and $\text{MnBi}_6\text{Te}_{10}$ were obtained. From this, it can be concluded that in the future, the modified Bridgman method can be used for the synthesis of $\text{MnIn}_x\text{Bi}_{y-x}\text{Te}_{1.5y+1}$ compounds.

Differential thermal analysis (DTA) of mixtures of $\text{Mn}(\text{In}_x\text{Bi}_{1-x})_2\text{Te}_4$ composition was performed to determine the crystallization temperature of these compounds. The DTA data showed that with an increase in the indium content, the crystallization temperature decreases by 1-2 °C for every 10 mole percent.

The synthesis of $\text{Mn}(\text{In}_x\text{Bi}_{1-x})_2\text{Te}_4$ crystals was performed using a modified Bridgeman method at temperatures obtained from DTA data. Diagnostics of the elemental and phase composition and grown single crystals was performed using the methods of XFS and XRD.

Transport properties of all synthesized $\text{Mn}(\text{In}_x\text{Bi}_{1-x})_2\text{Te}_4$ single crystals were investigated up to temperature of 50 mK. It was found that none of the synthesized crystals exhibit superconducting properties in the studied temperature range. It can be concluded that to achieve superconductivity, the indium content must be increased.

The band structure of the MnBi_2Te_4 indium-doped samples was studied by angle-resolved photoemission spectroscopy (ARPES). An increase of indium in the crystal leads to a proportional increase in the observed band gap. It can be assumed that in the $\text{Mn}(\text{In}_x\text{Bi}_{1-x})_2\text{Te}_4$ system is a topological – trivial insulator transition, and an increase in the observed band gap is associated with the appearance of impurity states of indium in it.

Two-dimensional Ferrovalley Semi-Half-Metal and Tunable Valley-Unbalanced Quantum Anomalous Hall Effect

Mu Tian¹, Run-wu Zhang^{1,*}

¹ Beijing Key Lab of Nanophotonics & Ultrafine Optoelectronic Systems, and School of Physics,

Beijing Institute of Technology, Beijing 100081, China

*email: tianmu@bit.edu.cn

Abstract

As a promising competitor for novel quantum devices, magnetic topological materials attract much attention in recent year for its interesting physical properties in magnetism and electron transport. In this work, we find a ferromagnetic topological material with a high Chern number of 2. Based on first principle calculations, we find 1T-CrS₂F₂ monolayer, which is halogenide of 1T-CrS₂ that has been successfully synthesized is stable at regular situation and possess intrinsic ferromagnetism as well as energy valleys. When spin-orbit coupling(SOC) is considered, the anomalous hall conductance appears as a quantum platform of $-2 e^2/h$ and two metallic edge states are discovered between valence band and conduction band. However, the presence of space inversion symmetry makes valleys equivalent and restrict further application. So a Janus structure 1T-CrS₂FCl is constructed to introduce energy valley polarization. After considering SOC in ferromagnetic 1T-CrS₂FCl, we can destroy the equivalence between energy valleys and apply a perpendicular electric field to tune the band structure. With electric field we can attain tunable QAH conductance. Our research provides are instructive for the discovery of magnetic topological materials and the research of novel spintronic devices.

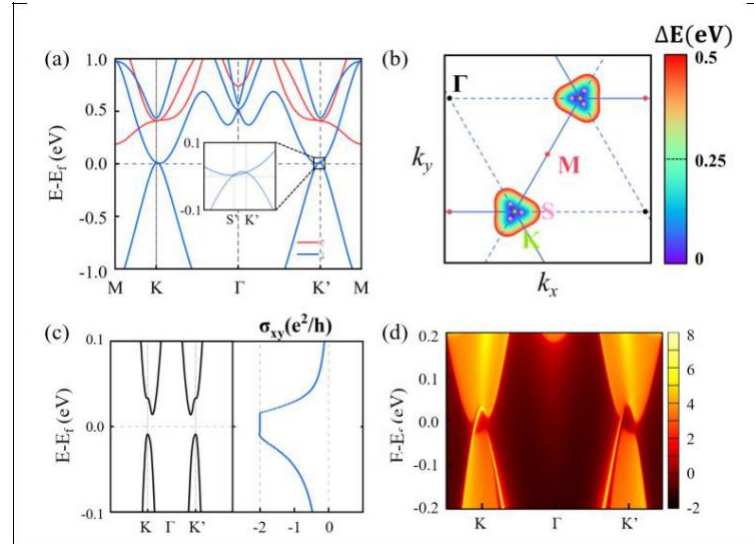


Fig.1 Electronic properties and topological properties of 1T-CrS₂F₂. (a) The spin-polarized band without considering SOC, and the inset shows the quadratic crossover between conduction and valence bands near K'.(b) The triangular warping structure in the ferromagnetic band. (c) Band structure and the quantum anomalous Hall effect of 1T-CrS₂F₂ with SOC considered. (d) Two metallic edge states between the conduction band and the valence band.

Microwave generator based on the Josephson junction

R. Tyumenev¹, D.S. Kalashnikov^{1,2}, A.G. Shishkin^{1,2}, V.S. Stolyarov^{1,2}

¹ Moscow Institute of Physics and Technology, Moscow, Russia

² N.L.Dukhov All-Russian Research Institute of Automation, Moscow, Russia *email: tyumenev.r@phystech.edu

Physical systems used for quantum computing operating in the microwave range require advanced control electronics, and the use of integrated components operating at the temperature of quantum devices is potentially beneficial.

In this paper, we consider a generator consisting of a Josephson junction, a microwave resonator, a shunt capacitance and a resistance. Such a generator operates at a temperature of 20 mK at a frequency corresponding to the control of qubits. The aim of the work is to determine the range of generator parameters in which stable generation is possible by numerical solution of the system dynamics equations, the manufacture of individual generator elements, as well as the search for its optimal parameters using modeling taking into account the obtained generator elements.

As a criterion for the appearance of alternating current generation, the condition described in [1], [2] was used. To calculate the impedance, the method proposed in [3] was used, in normalized values:

$$Z_w = R_w + jX_w = \left(\frac{1}{Ti_w} \right) \int_0^{T \rightarrow \infty} \phi e^{j\omega t} dt \quad (1)$$

As a result of this work, an analysis of the possibility of generation at different values of the McCumber parameters and the generator frequency normalized to the critical frequency of the Josephson transition is provided. During the work, samples of planar capacitors and normal resistance were manufactured and measured. Using the measured characteristics, the possibility of generating and the power of such a generator manufactured with a simpler planar technology is estimated using simulation.

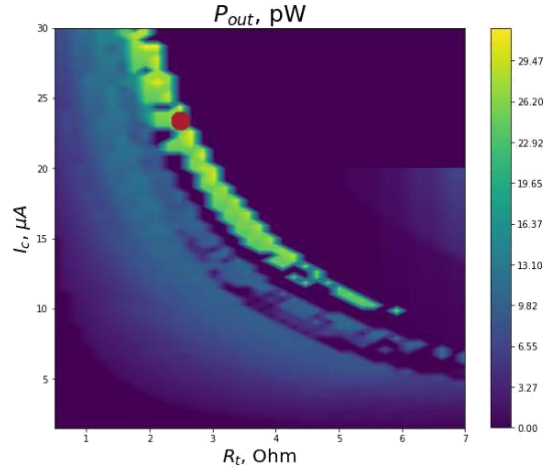


Fig. 1: The dependence of the AC generation power (indicated by color) on the actual system parameters obtained during operation. The maximum possible power is highlighted with a red dot.

Bibliography

- [1] *Chengyu Y., Juha H., Visa V., Jinli Z., Joni I., Leif G., Jan G., Mikko M.* A low-noise on-chip coherent microwave source. *Nature Electronics*. 2021. 885–892.
- [2] *Hassel J., Grönberg L., Helistö P., Seppä H.* Self-synchronization in distributed Josephson junction arrays studied using harmonic analysis and power balance. *Appl. Phys. Lett.* 2006. 89, 072503.
- [3] *Zhai Z., Parimi P. V., Sridhar S.* Nonlinear microwave impedance of short and long Josephson junctions. *Physical Review B* 59(14). 1999.

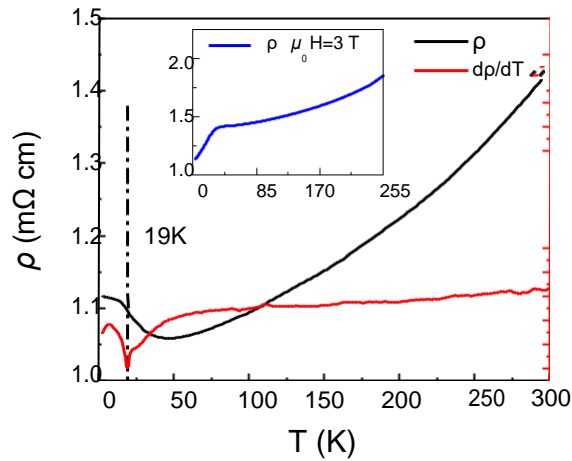
A new Mn-Bi-Te ternary antiferromagnetic topological insulator

Liu Yang^{1*}, ZhiWei Wang²

¹ Beijing Institute of Technology, Beijing, China

² Beijing Institute of Technology, Beijing, China *email: l_yang555@163.com

MnBi₂Te₄ antiferromagnetic topological has been attracted people's attention owing to its special surface states meanwhile its intrinsic magnetic^[1-3]. The gapless surface states of topological material expected to achieve quantum spin hall effect and further to attain lossless energy transport^[4]. But the temperature required to achieve quantum anomalous hall effect far below room temperature, due to material limitations, therefore, there is an urgent need to develop new topological insulators. In this work, we successfully growth Mn-Bi-Te ternary antiferromagnetic topological insulator by melting method and characterized using scanning transmission electron microscopy (STEM), Single Crystal X-Ray Diffraction (SXRD), physical property measurement system magnetic (PPMS) and Angle-resolved photoemission spectroscopy (ARPES). Novel Mn-Bi-Te ternary material belong to R3m space group, antiferromagnetic transition temperature is around 20K. When the magnetic field rises to 0.5T, a magnetic phase transition occurs which from antiferromagnetic to ferromagnetic. A amount of BiTe lead to P-type doped, so after evaporating cesium on the surface of the sample, the Fermi level can be seen to shift upwards through ARPES, thus revealing the surface state of the sample.



Pic.1 Resistance versus temperature curve of Mn-Bi-Te

Bibliography

- [1] Liu, Chang, Wang, et al. Nat. Mater. 19, 522–527 (2020)
- [2] Deng, Yujun, et al. Science 367, 895-900 (2020)
- [3] Zhang, Dongqin, et al. Phys. Rev. Lett. 122, 206401 (2019)
- [4] Yoichi Ando J. Phys. Soc. Jpn. 82, 102001 (2013)

Nanoscale visualization of symmetry-breaking electronic orders and magnetic anisotropy in a kagome magnet YMn_6Sn_6

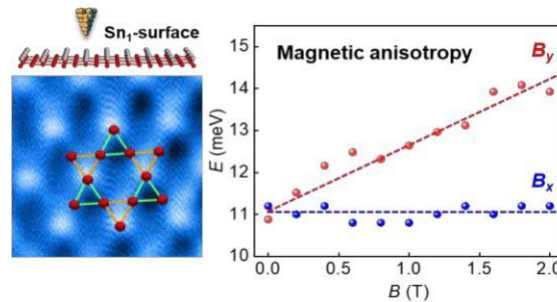
Can Zhang, Liangguang Jia, Yu Zhang^{*}, Yeliang Wang^{*}

School of Integrated Circuits and Electronics, MIIT Key Laboratory for Low-Dimensional Quantum Structure and Devices, Beijing Institute of Technology, Beijing, 100081

^{*}Email: yzhang@bit.edu.cn; yeliang.wang@bit.edu.cn

Kagome lattice hosts a plethora of quantum states arising from the interplay between nontrivial topology and electron correlations. The recently discovered kagome magnet RMn_6Sn_6 (R represents a rare-earth element) is believed to showcase a typical kagome band, with Dirac cones, flat bands, and Van Hove singularities located near the Fermi level. The Mn-Kagome layers dominate the nontrivial topological electronic properties of the crystal, while the R element significantly influences the magnetic structure. Therefore, the RMn_6Sn_6 family possesses numerous novel and tunable quantum properties^[1]. YMn_6Sn_6 , as one of its members, exhibits a spiral antiferromagnetic structure along the c-axis at low temperatures due to the non-magnetic Y^[2]. Investigating the kagome lattice electronic states and magnetization responses is crucial for understanding the unconventional electronic behaviors and complex magnetic phenomena arising from its unique geometric structure.

Here, we report the characterization of local electronic states and their magnetization response in YMn_6Sn_6 via scanning tunneling microscopy measurements under vector magnetic fields^[3]. Our spectroscopic maps reveal a spontaneously trimerized kagome electronic order in YMn_6Sn_6 , where the sixfold rotational symmetry is disrupted while translational symmetry is maintained, exhibiting correlation-driven unusual orbital textures. Further application of an external vector magnetic field demonstrates a strong coupling of the YMn_6Sn_6 kagome band to the field, which exhibits an energy shift discrepancy under different field directions, implying the existence of a magnetization-response anisotropy and anomalous g factors. Our findings establish YMn_6Sn_6 as an ideal platform for investigating kagome-derived orbital magnetic moment and correlated magnetic topological states.



Pic. 1 There exists a spontaneously trimerized kagome electronic order in YMn_6Sn_6 , and it exhibits anisotropic magnetic responses when external vector magnetic fields are applied in different directions.

Bibliography

- [1] Yin, J.; Lian, B.; Hasan, M. *et al. Nature* **2022**, **612**: 647.
- [2] Ghimire, N.; Dally, R.; Poudel, L. *et al. Sci. Adv.* **2020**, **6**: eabe2680.
- [3] Jia, L.[#]; Chen, Y.[#]; Zhang, Y.[#]. *et al. Nano lett.* **2024**, **24**: 8843.

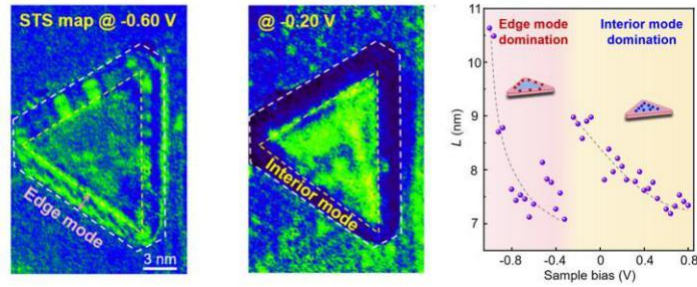
Intertwined quantum confinement effects in charge-density-wave nanostructures

Lili Zhou¹, Yu Zhang^{1*}, and Yeliang Wang^{1*}

¹Beijing Institute of Technology, Beijing 100081, China.

*email: yzhang@bit.edu.cn; yeliang.wang@bit.edu.cn

Charge carriers confined into a geometrical configuration approaching the nanoscale are expected to show remarkable confinement phenomena that depart from the intrinsic ground states. Especially for the many-body interacting systems, understanding the underlying physics of quantum confined behaviors at the atomic scale is critical for the advancement of nanoscience and nanotechnology. Here we report anomalous quantum confinement effects and modulation effects of the substrates in triangular-like nanostructures of monolayer H-NbSe₂ by scanning tunneling microscopy experiments. The monolayer H-NbSe₂ nanostructures on graphene substrates usually generate domain boundaries which disappear when the substrates are H/T-NbSe₂. Moreover, both H-NbSe₂ and T-NbSe₂ substrates can effectively induce striped charge states in monolayer H-NbSe₂ nanostructures. More importantly, our spectroscopic measurements reveal remarkable electron confinement behaviors in monolayer H-NbSe₂ nanostructures on H-NbSe₂ substrates, where the confined electrons can be visualized either along the nanostructure edges or within the nanostructures, dependent on the electron energies, resulting in intertwined quantum confinement effects, which are anomalous quantum confinement effects. Our results provide a fruitful playground for investigating the intertwined quantum confinement effects in charge-density-wave nanostructures under the two-dimensional limit.



Bibliography

- [1] Y. Y. Chen, Y. Zhang, W. Wang, Y. L. Wang, et al. Adv. Sci. 2306171, 1 (2023).
- [2] Q. Z. Zhang, Y. Zhang, Y. H. Hou, Y. L. Wang, et al. Nano Lett. 22, 1190 (2022).

Crystal growth of topological insulators with bulk-insulating property

Peng Zhu^{1, 2, 3}, Zhiwei Wang^{1, 2, 3} *

1. Centre for Quantum Physics, Key Laboratory of Advanced Optoelectronic Quantum Architecture and Measurement (MOE), School of Physics, Beijing Institute of Technology, Beijing 100081, China
2. Beijing Key Lab of Nanophotonics and Ultrafine Optoelectronic Systems, Beijing Institute of Technology, Beijing 100081, China
3. Material Science Center, Yangtze Delta Region Academy of Beijing Institute of Technology, Jiaxing, 314011, P. R. China

*email: zhiweiwang@bit.edu.cn

Topological insulators (TIs) represent a novel quantum state of matter, characterized by an insulating bulk property and a conducting edge or surface state that protected by time-reversal symmetry [1, 2]. This topological surface state gives rise to numerous exotic transport phenomena, including Shubnikov-de Haas (SdH) oscillations, anti-weak localization and the quantum Hall effect (QHE) [3, 4], etc. In three-dimensional (3D) TIs, the two half-integer quantized Hall conductances from the top and bottom surfaces collectively contribute to the integer quantized Hall conductance. The Bi₂Se₃ family, including Bi₂Se₃, Bi₂Te₃, and Sb₂Te₃, is considered an ideal class of 3D TIs [5]. However, these materials often have poor bulk insulating property due to the presence of vacancies and anti-site defects. Thus, the bulk-dominated transport induces significant challenge in observing the QHE in 3D TIs [3, 6, 7].

Bi_{2-x}Sb_xTe_{3-y}Se_y displays an amazing low carrier density, especially for the composition of $x=1$ and $y=2$, that is BiSbTeSe₂. The surface mobility was improved to 4000 cm²/Vs through a two-step melting-Bridgman growth[8]. On this basis, we further improved the surface mobility to 7000cm²/(Vs) in device and realized QHE without gating. Besides, we observed a bulk insulating behavior in Bi₂Te₃ derived from topological superconductor candidate Tl_{0.6}Bi₂Te₃ through increasing Te content.

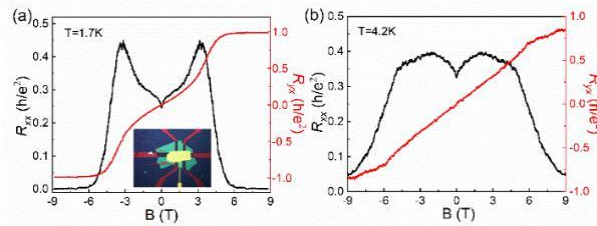


Fig. 1 QHE of Sn_{0.02}Bi_{0.98}SbTeSe₂ device without gating.

Bibliography

- [1] Hasan M Z and Kane C L. *Reviews of Modern Physics* **2010**, 82 (4), 3045.
- [2] Ando Y. *Journal of the Physical Society of Japan* **2013**, 82 (10), 102001.
- [3] Cao H, Tian J, Miotkowski I, Shen T, Hu J, Qiao S and Chen Y P. *Physical Review Letters* **2012**, 108 (21), 216803.
- [4] Bao L, He L, Meyer N, Kou X, Zhang P, Chen Z-g, Fedorov A V, Zou J, Riedemann T M, Lograsso T A, Wang K L, Tuttle G and Xiu F. *Scientific Reports* **2012**, 2 (1), 726.
- [5] Zhang H J, Liu C X, Qi X L, Dai X, Fang Z and Zhang S C. *Nature Physics* **2009**, 5 (6), 438.
- [6] Analytis J G, Chu J-H, Chen Y, Corredor F, McDonald R D, Shen Z X and Fisher I R. *Physical Review B* **2010**, 81 (20), 205407.
- [7] Checkelsky J G, Hor Y S, Cava R J and Ong N P. *Physical Review Letters* **2011**, 106 (19), 196801.
- [8] Han K B, Chong S K, Oliynyk A O, Nagaoka A, Petryk S, Scarpulla M A, Deshpande V V and Sparks T D. *Scientific Reports* **2018**, 8 (1), 17290.

Vortex glass – vortex liquid phase transition in the iron-based superconductor PrFeAs(O,F)

I.V.Zhuvagin^{1,2*}

¹ Lebedev Physical Institute, Russian Academy of Sciences, 119991, Moscow, Russia ² HSE University, 101000, Moscow, Russia

*email: i.zhuvagin@lebedev.ru

The study of vortex dynamics [1] is an important scientific task related to the observation of new states of matter and also technologically promising. The oxypnictides $\text{ReFeAsO}_{1-x}\text{F}_x$ (Re = rare-earth elements) is one of the most high-temperature families among iron-based superconductors. In this work, the vortex glass - vortex liquid phase transition in the single crystal $\text{PrFeAsO}_{0.6}\text{F}_{0.35}$ is studied. The temperature dependences of resistivity and current-voltage characteristics were obtained with an applied magnetic field up to 16T along the c axis. The significant broadening of superconducting transition and the tail in the resistivity curve before reaching zero resistivity are signs of the presence of strong thermal fluctuations in the system. The magnetic dependences of critical exponent for the vortex-glass scaling [2] and the thermal activation energy [3] demonstrate crossover (3D - 2D) for magnetic field around 4T.

[1] Blatter G. et al., Reviews of modern physics, 1994.

[2] M.P.A. Fisher, Phys. Rev. Lett, 62, 1415, 1989.

[3] Arrhenius S.A., Z.Phys.Chem. 4, 1889.

Implementation of a fast qubit reset algorithm on a superconducting transmon.

A. A. Solovev^{1,2}, A. V. Lebedev^{1,2}

¹*Moscow Institute of Physics and Technology (MIPT), Dolgoprudny, 141700, Russia*

²*Dukhov Research Institute of Automatics (VNIIA), Moscow, 127030, Russia*

The task of fast initializing a qubit circuit is one of the most important challenges in the implementation of quantum computing. According to the DiVincenzo criteria for realizing quantum computation, it is essential to be able to prepare the initial state, which in all algorithms traditionally corresponds to the ground state of the quantum system.

There are several methods for accomplishing this procedure. The main approaches for superconducting qubits are: measuring the system with subsequent application of corrective pulses depending on the measurement outcome, and stimulated decay via the readout resonator. The second method is used in this work. To bring the qubit to the ground state, the protocol utilizes a transition between levels of the qubit-resonator system operating in the dispersive regime. Specifically, the level corresponding to the second excited state of the qubit with no photons in the resonator and the level corresponding to the ground state of the qubit with one photon in the resonator are used.

The fast initialization protocol consists of the following pulse sequence: first, a π -pulse is applied to the qubit to transition between the first and second excited states. Then, a signal is applied to the qubit at the difference frequency corresponding to the levels $|2\rangle \otimes |0\rangle$ and $|0\rangle \otimes |1\rangle$, where the notation $|\text{qubit}\rangle \otimes |\text{resonator}\rangle$ is used. Thus, due to the effect of Rabi oscillations, the system is transferred to the $|0\rangle \otimes |1\rangle$ state, after which the photon decays from the resonator in a time much shorter than the qubit's lifetime, ensuring fast initialization. Additionally, during excitation of this transition, resonant pumping at the $|1\rangle - |2\rangle$ transition frequency of the qubit is applied to compensate for decay effects.

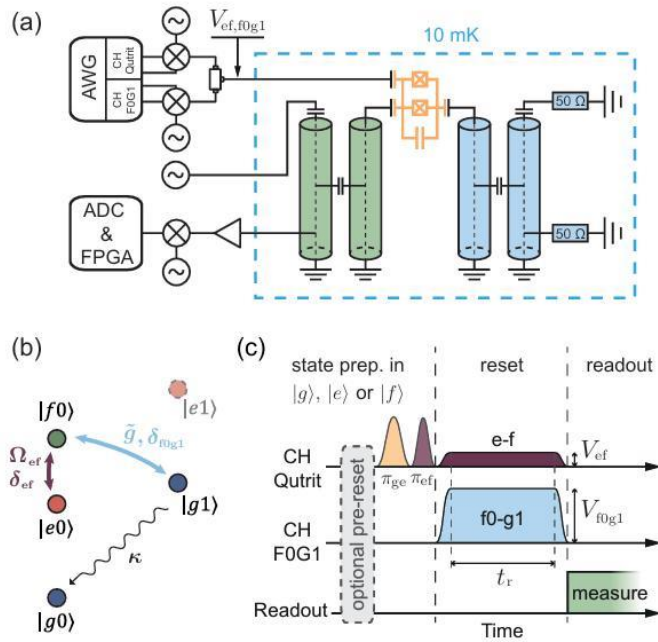


Figure 1. Schematic diagram of the fast initialization protocol [2].

This work demonstrates the experimental implementation of this protocol on transmons, showing a reduction in qubit initialization time from 200 μs to 5 μs . For further improvement, it is necessary to increase the coupling strength between the qubit and the resonator and to use a Purcell filter.

References:

1. Koch, J., Yu, T. M., Gambetta, J., Houck, A. A., Schuster, D. I., Majer, J., ... & Schoelkopf, R. J. (2007). Charge-insensitive qubit design derived from the Cooper pair box. *Physical Review A—Atomic, Molecular, and Optical Physics*, 76(4), 042319.
2. Magnard, P., Kurpiers, P., Royer, B., Walter, T., Besse, J. C., Gasparinetti, S., ... & Wallraff, A. (2018). Fast and unconditional all-microwave reset of a superconducting qubit. *Physical review letters*, 121(6), 060502.

Design of a transmon qutrit scheme for quantum magnetometry.

T. A. Yaropolov^{1,2}, A. V. Lebedev^{1,2}

¹*Moscow Institute of Physics and Technology (MIPT), Dolgoprudny, 141700, Russia*

²*Dukhov Research Institute of Automatics (VNIIA), Moscow, 127030, Russia*

Quantum magnetometry is a rapidly advancing field that leverages quantum systems to achieve sensitivity levels beyond the standard quantum limit, approaching the Heisenberg limit through the use of quantum resources (coherence and entanglement). One promising platform for quantum sensors is the superconducting transmon [1], which offers artificial atoms with a large magnetic moment controlled by microwave signals. Recent theoretical work [2] has shown that exploiting higher-dimensional quantum systems, such as qutrits (three-level systems), can further increase the phase estimation efficiency and expand the dynamic range of quantum sensors.

This work focuses on the design and modeling of a scalable transmon-based qutrit quantum circuit specifically optimized for quantum magnetometry applications. The core of the developed architecture consists of nine frequency-tunable transmon qutrits, each capacitively coupled to an individual coplanar waveguide (CPW) resonator and equipped with a dedicated DC bias line for magnetic flux tuning. The transmon qutrits are engineered with optimal anharmonicity to separate the fundamental and next-excited state transitions (ω_{01} and ω_{12}) within a 5–6 GHz range, minimizing frequency crowding and enhancing addressability. The resonance frequencies of the CPW cavities (6.6–6.9 GHz) and their quality factors are optimized to enable high-fidelity dispersive readout while maintaining low loss and minimal cross-talk between channels. Capacitively engineered coupling ensures strong readout signal contrast and preserves coherence properties.

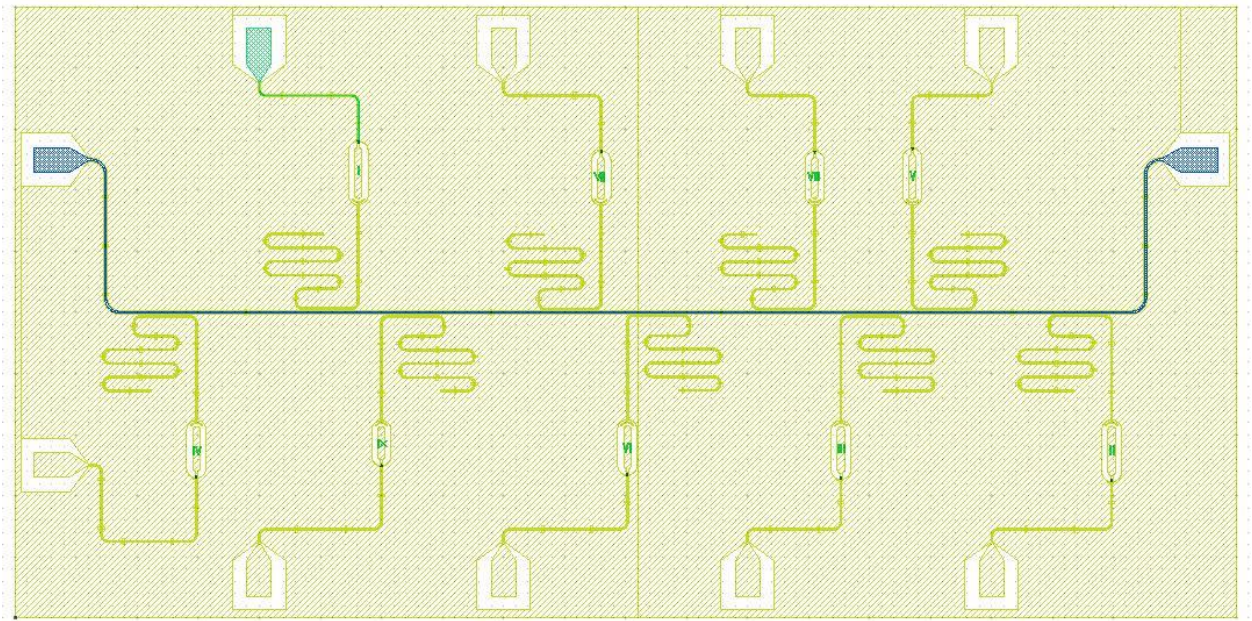


Figure 1. Schematic representation of a qutrit quantum circuit consisting of nine transmons, individual quarter-wavelength coplanar resonators, a common readout line, and DC control lines.

Numerical simulations and analytical calculations of the proposed device include estimation of transition frequencies, anharmonicities, coupling strengths, and the relationship between the flux-bias currents and the energy levels of the qutrits. Special attention is given to the relationship between circuit design parameters and the achievable magnetic sensitivity, as well as potential operation points offering maximal coherence or optimal metrological performance.

The results lay the groundwork for the practical use of transmon qutrits as quantum sensors for weak magnetic fields and demonstrate the feasibility of scalable multiqutrit architectures for quantum-enhanced metrology. The developed scheme may serve as a prototype of a next-generation quantum magnetometer, capable of realizing advanced phase estimation protocols and approaching the Heisenberg limit for measurement sensitivity.

References:

1. Koch, J., Yu, T. M., Gambetta, J., Houck, A. A., Schuster, D. I., Majer, J., ... & Schoelkopf, R. J. (2007). Charge-insensitive qubit design derived from the Cooper pair box. *Physical Review A—Atomic, Molecular, and Optical Physics*, 76(4), 042319.
2. Shlyakhov, A. R., Zemlyanov, V. V., Suslov, M. V., Lebedev, A. V., Paraoanu, G. S., Lesovik, G. B., & Blatter, G. (2018). Quantum metrology with a transmon qutrit. *Physical Review A*, 97(2), 022115.